Regular Article

Design, Synthesis and Screening of 4,6-Diaryl Pyridine and Pyrimidine Derivatives as Potential Cytotoxic Molecules

Mohammed K. Abd elhameid,*[,a] Noha Ryad,[b] Al-Shorbagy MY,[c,d] Manal R. mohammed,[e] Mohammed M. Ismail,[a,b] and Salwa El Meligie[a]

[a] *Pharmaceutical Organic Chemistry Department, Faculty of Pharmacy, Cairo University; Cairo 11561, Egypt:* [b] *Pharmaceutical Organic Chemistry Department, College of Pharmaceutical Sciences and Drug Manufacturing, Misr University for Science and Technology; Giza P.O.Box 77, Egypt:* [c] *Pharmacology and Toxicology Department, Faculty of Pharmacy, Cairo University; Cairo 11561, Egypt:* [d] *School of pharmacy, Newgiza University; Giza 12566, Egypt: and* [e] *Department of Radiation Biology, National Center for Radiation Research and Technology; Cairo 11787, Egypt.*

Received April 7, 2018; accepted July 20, 2018; advance publication released online August 14, 2018

A new series of pyridine and pyrimidine derivatives is designed and synthesized as potential antitumor molecules. The tested compounds show promising *in vitro* cytotoxic activity against HL-60 cell line as eight compounds: 4, 6, 11, 13, 14, 15, 18 and 21 exhibit potent cytotoxic activity in sub-micromolar concentration higher than the combretastatin A4 (CA-4). Compound 21 shows a cytotoxic activity 5- fold more potent than CA- 4 on HL-60 cells. DNA-Flow cytometry cell cycle analysis and annexin-V assay on HL-60 cells show that compounds 4, 18 and 21 exhibit potent cell growth inhibition, cell cycle arrest at G_2/M phase and pro-apoptotic inducing activities. The percentage inhibition assay of *β*-tubulin polymerization on HL-60 cells shows that the antitumor activity of the tested compounds appears to correlate well with its ability to inhibit *β*-tubulin polymerization. In addition, enzyme-linked immunosorbene assay (ELISA) measurement for com-pound 21 shows apoptotic inducing activities through significant up regulation of p53, Bax/Bcl-2 ratio and caspase-3 proteins parallel to down regulation of the level of survivin proteins.

Key words pyridine; pyrimidine; leukemia; survivin; tubulin; combretastatin A4

Cancer is a major health dilemma all over the world.[1)] Leukemia is a type of cancer that affects the blood and bone marrow and considered as one of the most life threatening agent to human.[2)] In the last decade, target based chemotherapy drugs are developed for treatment of cancer to overcome the drawbacks of conventional chemotherapy.[3)] Microtubules synthesis is considered one of the main target for the natural lead cytotoxic compounds as colchicine and etoposide (Fig. 1). These drugs act by inhibiting tubulin polymerization into microtubules. They act as catalytic inhibitors on the binding sites of tubulin leading to inhibition of microtubules assembly and prevent the formation of the mitotic spindle in the mitosis and consequently, mitotic cell death (MCD).[4–6)] The classical antimitotic drugs are highly successful in the control of cancer cells growth, especially tumor cells with high mitotic index.[7)] The different binding sites of antimitotic drugs are known as colchicine and vinca alkaloids binding sites.[8,9)] Resistance of cancer cells to apoptosis induction by antimitotic drugs leads to increase in the used dose of the drugs which also, increase side effects and drawbacks of these drugs.[10,11)]

Combretastatin-A4 (CA-4) (Fig. 1) is one of the naturally potent newer MCD targeting drugs. The main clinical drawback of CA-4 that limits its use is *cis- trans* isomerization.[12)] Several reported studies published to solve the structural problem based on the synthesis of rigid isosteric analogues containing pyridine and pyrimidine rigid core rings **I**–**V**, as structural modification instead of ethylene bridge (Fig. 1).[13–15)] Our research group is interested in synthesis of different rigid analogues of CA-4.[15–18)] The reported 2, 6-diarylpyridines **I**–**III** and 4, 6-diaryl pyrimidines **IV** and **V** show a remarkable anti-proliferative activity against different cancer cell lines, such as breast cancer MCF-7 cells and colon cancer HCT-116 cells. The promising cytotoxicity is explained by keeping the common pharmacophoric structural as colchicine and CA-4.[19)] The structural basis for the cytotoxic action of these antimitotic compounds **I**–**V** are a triarylated ring system represented by two aryl rings (**A**) and (**C**) decorated with methoxy/hydroxyl groups similar to the aryl rings of CA-4 and colchicine linked *via* rigid core rings (**B**). Furthermore, survivin protein is a member of inhibitors of apoptosis proteins (IAPs), it has a dual biological actions in the resistance of cancer cells to antitumor agents by suppressing induction of cancer cells to apoptosis and promoting cell growth as mitotic facilitator.[20,21)] Survivin is highly expressed in leukemia and almost all types of cancer cells.[22–24)] Interestingly, by literature searching for chemical scaffolds acting as survivin inhibitors, it is found that 3-cyano-4,6-diaryl-2-pyridone derivatives **VI** and **VII** (Fig. 1) possess anticancer activity due to their ability to act as survivin inhibitors.[25)] Undoubtedly, the need to bridge the gap between minimizing side effects and the mode of action of antimitotic drugs encourage us for further investigations towards the synthesis of novel potent cytotoxic compound.[26,27)]

Structural analysis for both mentioned compounds, as antimitotic **I**–**V** and survivin inhibitors **VI** and **VII** , shows, regardless the positions of coupled two aryl groups (**A**) and (**C**) either at C-2, C-6 or at C-2, C-4 of the core rings (**B**), the structural skeleton as non-fused triarylated ring system is similar, as both pharmacophores are composed of pyridine or pyrimidine core rings and two other aryl rings directly connect-ed without spacer (Fig. 2). Based on aforementioned findings, three pharmacophoric models **A**, **B** and **C** are generated from common template formed from tricyclic ring system (Fig.

* To whom correspondence should be addressed. e-mail: mohorganic@hotmail.com

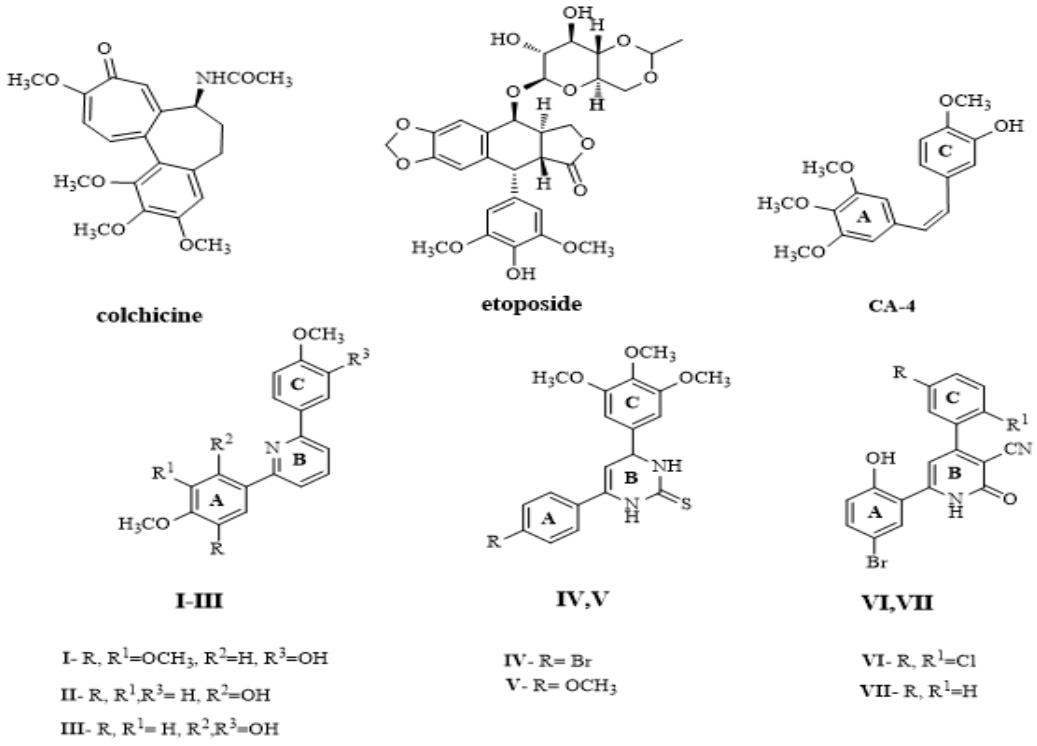

Fig. 1. Chemical Structures of Some Natural Mitosis Inhibitors (Colchicine and Etoposide), CA-4, Diaryl Pyridine **I**–**III**, **VI**, **VII** and Diaryl Py-rimidine Derivatives **IV**, **V** as Antimitotic Agents and Survivin Inhibitors

First aryl rings **A**, Core rings **B** represented by pyridine and pyrimidine moieties, the third aryl rings **C**, and pharmacophoric groups responsible for survivin inhibition.

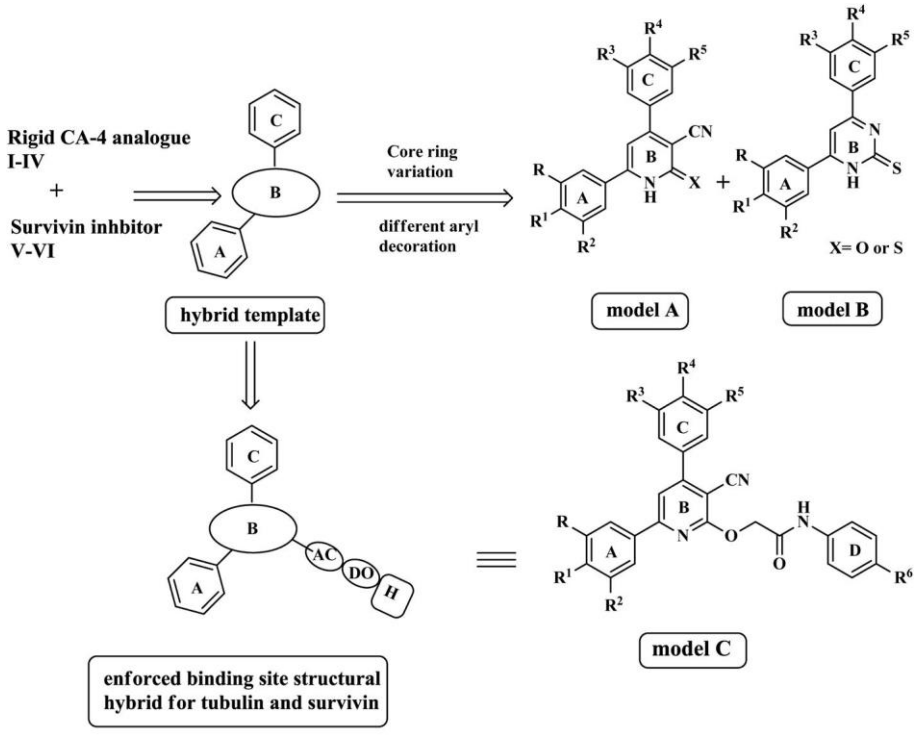

Fig. 2. Diagrammatic Sketch for Design Strategy of the Elucidated Lead Template and the Generated Three Hybrid Structural Model **A**, Model **B**, Model **C**, Where Triaryl Ring System Represent as Core Ring (Ring **B**), Aryl Ring Present in C-6 of the Core (Ring **A**) and C-4 Aryl (Ring **C**)

N-Aryl acetamide groups as hydrophobic hydrogen bond donner acceptor moieties that increased binding affinity.

2). The required three essential pharmacophoric features of colchicine site inhibitors (CSI) are present in the main structural template.[28–30] The structural variation between the three models is the change in the core rings either as 2-oxopyridine and 2-thioxopyridine, as in model **A** or 3-pyrimidinthione, as in model **B**. In addition, a second variation is present in the structural extension of the model **A** with hydrophobic hydro-gen bond acceptor-donor pair fragments, as in model **C**. The model **A** (Fig. 2) is designed as the prototype structure with pyridine core ring representing a common part in the reported survivin and *β*-tubulin polymerization inhibitors. Further-more, in model **A**, the pyridine ring is reinforced with *ortho*-oxo or thioxo-cyano functional groups present in survivin inhibitors. Both aryl arms of the core ring are decorated with 4-methoxyphenyl, hydroxy methoxyphenyl and 3, 4, 5-trime-thoxyphenyl (TMP) groups similar to the ones present in the CA-4, and colchicine. Moreover, isosteric replacement of the pyridine ring core by pyrimidine ring as in the reported cytotoxic compounds **IV** and **V** that show promising antitumor activities lead to generation of pharmacophoric model **B** (Fig. 2).

In recent reports, the docking study results of CSI show that there are 7-pharmacophoric structural features for the binding between the receptor site and CSI drugs and to the best of our knowledge, none of the present CSI compounds have all of the 7- pharmacophoric features.[28–30] This finding motivates us to design a third model **C**. The pharmacophoric model **C** is designed by grafting the structure of model **A** with *N*-aryl acetamide groups at C-2 of pyridine ring, as hydrophobic and hydrogen bond acceptor-donner pair groups, to increase pharmacophoric binding features towards binding site (Fig. 2). The therapeutic target of this rational design is to increase cytotoxic and to enhance pro-apoptotic activities of the novel compounds towards tumor cells. This tactic is the most efficacious therapeutic strategy to increase cytotoxic properties of the chemotherapeutic agents and decrease their side effects.[31]

Results and Discussion

Chemistry Sustainable development in organic chemistry is a growing target for all chemists in order to improve synthetic protocols for building up novel synthetic compound

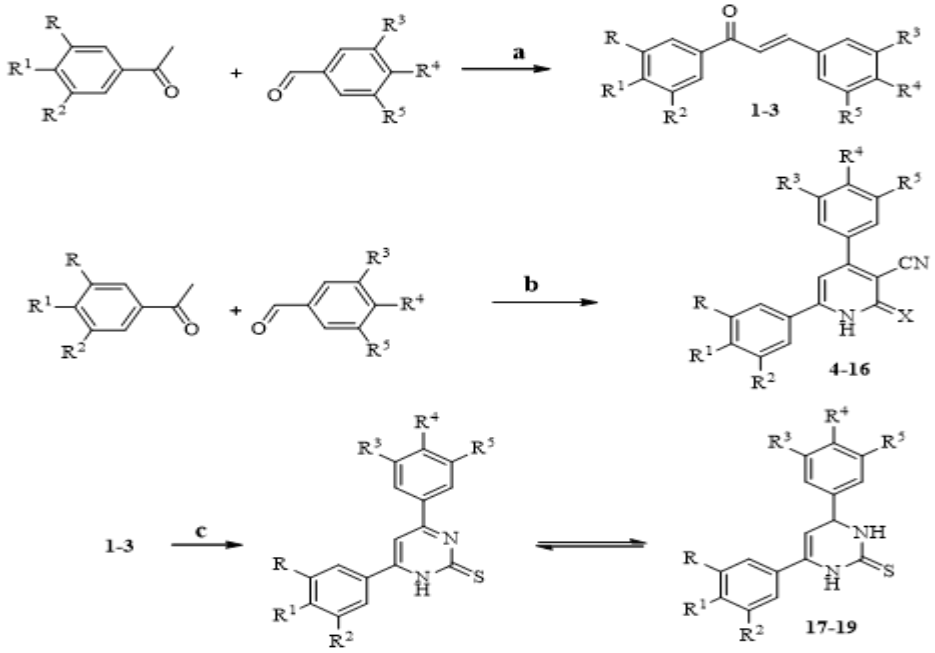

1-R, R^2 = H , R^1 , R^3, R^4, R^5 = OCH_3
2-R, R^I, R^2, R^5 = OCH_3 , R^3= H , R^4= OH
3-R, R^I , R^2 ,R^3 , R^4, R^5 = OCH_3
4-X= S, R, R^I , R^2, R^4 =OCH_3 , R^3 , R^5 =H
5-X= S, R, R^I , R^2 , R^3 , R^4 , R^5 =OCH_3
6-X= S, R, R^I , R^2 , R^5 = OCH_3, R^4= OH, R^3 =H
7-X= S, R, R^2 = H , R^1 , R^3 , R^4 ,R^5 = OCH_3
8-X= S, R, R^2 , R^3 , H , R^4= OH , R^1 = R^5= OCH_3
9-X= S, R, R^2= H, R^1= OH , R^3, R^4, R^5 =OCH_3
10-X= S, R, R^2, R^3 = H, R^1,R^4=OH, R^5= OCH_3

11-X = O, R, R^I, R^2 , R^4 = OCH_3 , R^3 , R^5 =H
12-X= O, R, R^I, R^2 , R^3, R^4, R^5 = OCH_3
13-X= O, R, R^I,R^2 , R^5 = OCH_3, R^4= OH, R^3 =H
14-X= O, R, R^2 = H ,R^1, R^3 , R^4, R^5 =OCH_3
15-X= O, R, R^2, R^3 = H, R^4= OH , R^1=R^5= OCH_3
16-X= O, R, R^2 = H , R^1= OH , R^3, R^4 , R^5 = OCH_3
17-R, R^2 = H, R^1 , R^3 , R^4, R^5 = OCH_3
18 -R^I, R^2, R^4= OCH_3, R^3 =H, R^5 = OH
19-R, R^I , R^2 , R^3 , R^4 ,R^5= OCH_3

Reagents and conditions: a) ethanolic 5% NaOH, stirring, 2h, b) cynanothioacetamide, ethyl cyanoacetate, ammonium acetate, *n*-butanol, stirring, min, 150°C M.W. 5–10 min, thiourea, sodium ethoxide, ethanol, 110°C, M.W., 10 min.

Chart 1. Synthesis of 3-Cyano-4,6-diaryl-2-pyridinthione Derivatives **4**–**10**, 3-Cyano-4,6-diaryl-2-pyridinone Derivatives **11**–**16** and 4,6-Diaryl-3-pyrimidinthione Derivatives **17**–**19**

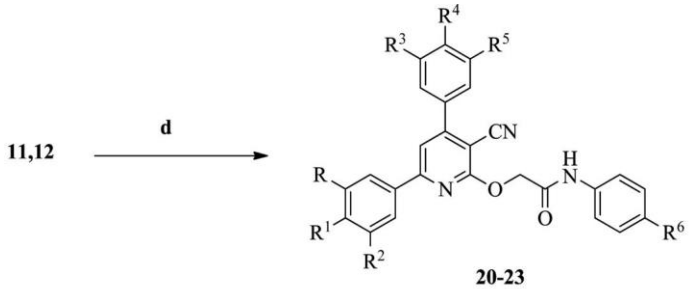

20-R, R^1, R^2, R^4= OCH_3 , R^3, R^5 , R^6 =H

21-R, R^1, R^2, R^4, R^6= OCH_3 , R^3, R^5 =H

22-R , R^1, R^2 , R^3, R^4, R^5 = OCH_3 , R^6 =H

23-R , R^1, R^2, R^3, R^4 , R^5, R^6 = OCH_3

Reagents and conditions: d) *N*-aryl chloroacetamides, anhydrous potassium carbonate, ethanol, 100°C M.W., 15 min.

Chart 2. Synthesis of 2-(3-Cyano-4,6-diarylpyridin-2-yl) oxy)-*N*-aryl Acetamides **20**–**23**

libraries. Microwave-assisted organic synthesis (MWAOS) is a branch of green chemistry which used in sustainable synthesis and has many advantages over conventional heating methods, such as being pollution free and eco-friendly.[32] Recently, two synthetic microwave-assisted synthesis methodologies are established, open vessel microwave-assisted organic synthesis (OVMAOS), and closed vessel microwave-assisted organic synthesis (CVMAOS). The former has the advantages of being safe and could be used in a large scale, which is suitable for industrial chemistry.[33] OVMAOS methodology is used herein in the synthesis of final compounds **4**–**23**. The synthetic steps included in the preparation of starting materials, intermediates and the target compounds **4**–**23** are illustrated in (Charts 1 and 2). The required starting materials **1**–**3** are prepared by condensation of aromatic aldehydes with substituted acetophenones under basic conditions (ethanolic sodium hydroxide solution), as reported.[34,35]

Literature reports show that pyridine derivatives could be prepared using two synthetic pathways either by cyclization in one pot reaction *via* reaction of respective aldehydes, ketones, active methylene derivatives (ethylcyanoacetate or cyanoacetamide) and excess ammonium acetate, or, in two steps, *via* heating aldehydes and ketones to form chalcone derivatives then reacting the prepared chalcones with active methylenes in basic medium.[36–38] The 2-pyridinthiones **4**–**10** and isosteric 2-pyridinones **11**–**16** are prepared herein by one pot four component-reaction, by reacting equimolar amount of appropriate aromatic aldehydes, substituted acetophenones, cyanothioacetamide or ethyl cyanoacetate and excess of ammonium acetate (Chart 1). The reaction mixture is irradiated in high boiling solvent, such as *n*-butanol. The cyclization of the reacting materials into corresponding 3-cyano-2-pyridin-thione derivatives **4**–**10** is confirmed by its ^{1}H-NMR spectrum that displayed a singlet at δ 6.88 ppm for the CH proton of pyridine, while its ^{13}C-NMR spectrum also revealed signals at δ 117.6 and 161.8 ppm for nitrile and thiocarbonyl groups, respectively. The isomeric cyano-2-pyridinones **11**–**16** are prepared at low temperature and short reaction time than corresponding cyano-2-pyridinhiones. Its ^{1}H-NMR spectrum displays a singlet at δ 6.97 ppm for the CH proton of pyridine ring and a broad D_2O exchangeable singlet at δ 12.69 ppm for the NH proton. Compounds **13** and **15** are reported[39] under conventional heating in low yields compared with that of microwave-assisted synthesis method. Furthermore, the reported data characterized compounds **13** and **15** only without any biological screening.

Condensation of chalcones with thiourea under basic conditions, to afford the corresponding 3-pyrimidinthione is reported.[15,40–42] In the present work, chalcone derivatives **1**–**3**, when heated with thiourea in presence of sodium ethoxide as basic catalyst for 5 min, under microwave-assisted conditions, give the corresponding 3,4-dihydropyrimidine-2-(1*H*) thiones. Proton spectra of compounds **17** and **18** show two doublets in the regions 5.04, 5.41 ppm correlated to the neighboring methine and methylene protons of pyrimidine. Condensation of chalcone derivative **3** with thiourea require a longer reaction time (15 min) to obtain the pyrimidine derivative **19**. The structure of the obtained product is 2-pyrimidinhione and not 3,4-dihydropyrimidine-2-(1*H*) thiones (Chart 1). The structure of the pyrimidine derivative **19** is confirmed by ^{1}H-NMR spectra that display a singlet peak of methylene protons of pyrimidine at 7.74 ppm and devoid the two doublets correlated to the neighboring methine and methylene protons of pyrimidine. Compound **17** is previously prepared under conventional heating with the same physical and spectral data.[15] Several synthetic trails are performed to prepare 3-pyrimidinone derivatives, using urea, however, unfortunately, all cyclization trails are unsuccessful. Alkylation of the 3-cyano-2-pyridi-nones **11** and **12** with different *N* -aryl acetamide derivatives using ethanol as a solvent and in the presence of anhydrous K_2CO_3 results in synthesis of ether derivatives **20**–**23** (Chart 2). The structure of the products is elucidated by ^{1}H-NMR spectra that showed singlet peak of 2H of methylene protons of the side chain at 5.19 ppm, and by ^{13}C-NMR that shows peak at 66.02 ppm, revealed to methylene carbon of the chain. Furthermore, 2D analysis for compound **23** (Heteronuclear Multiple Bond Correlation (HMBC) is carried out and shows a key correlation of the proton signal at δ 5.17 (CH_2) to ^{13}C signals at δ 163 (C-2 of 3- cyanopyridine ring) and absence of correlation to ^{13}C signals at δ 157 (C-6 of cyanopyridine ring), indicating that alkylation is performed with oxygen and not nitrogen atoms. Similar synthetic procedures are performed to alkylate 3-cyano-2-pyridinthione derivatives **4**–**10**, however, these experimental trails failed to prepare thioether derivatives.

Biological Results and Discussion

In Vitro Cytotoxic Activity of Compounds **4**–**23** over HL-60, MCF-7 and HCT-116 Cancer Cell Lines

The cytotoxic activity of the synthesized compounds **4**–**23** is evaluated against three human tumor cancer cell lines, leu-

kemia HL-60 cells, breast cancer MCF-7 cells, and colon cancer HCT-116 cells, using 3-[4,5-dimethylthiazol-2-yl]-2,5-diphenyltetrazolium bromide (MTT) assay, as described.[43] The tested cancer cell lines are chosen for the following reasons: HL-60 leukemic cells are an excellent *in vitro* models for apoptosis studying assay.[44,45] Further, the reported lead structures **IV**, **V** showed a good cytotoxic activity against MCF-7 lines.[15] CA-4 is included in the experiment as po-tent antimitotic standard drug for the study against HL-60, MCF-7 and HCT-116 cancer cells (IC_{50} :0.48, 0.04 and 1 μM) respectively). The results of the mean values of four experiments performed, expressed as IC_{50} values, are summarized in (Tables 1–3). Analysis of cytotoxicity results against three cancer cell lines shows the following experimental observations. Cytotoxicity results over HL-60 cells, compounds **4** and **21** with IC_{50} (0.19 and 0.09 μM) are more potent by 2- and 5-fold higher than CA-4 (0.48 μM), respectively. Six pyridine derivatives, **4**, **6**, **11**, **13**, **14** and **15**, pyrimidinthione derivative **18** and ether derivative **21** (IC_{50} values ranging from 0.19 to 0.47 μM) are more potent than control drug, meanwhile the

Table 1. *In Vitro* Cytotoxic Activity (IC_{50} μM) of the Compounds **4**–**16** over HL-60, MCF-7 and HCT-116 Cancer Cell Lines

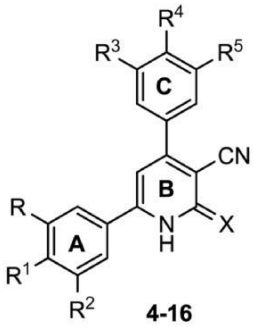

4-16

Comp No.	R	R^1	R^2	R^3	R^4	R^5	(IC_{50} μM)[a]		
							HL-60[b]	MCF-7[c]	HCT-116[d]
4	OCH_3	OCH_3	OCH_3	H	OCH_3	H	0.19±0.02	0.13±0.012	3.97±0.38
5	OCH_3	OCH_3	OCH_3	OCH_3	OCH_3	OCH_3	9.21±0.81	0.30±0.02	65.6±6.31
6	OCH_3	OCH_3	OCH_3	H	OH	OCH_3	0.21±0.03	2.19±0.17	0.48±0.05
7	H	OCH_3	H	OCH_3	OCH_3	OCH_3	0.50±0.04	0.21±0.02	5.91±0.60
8	H	OCH_3	H	H	OH	OCH_3	29.61±3.12	19.0±1.80	6.71±0.56
9	H	OH	H	OCH_3	OCH_3	OCH_3	23.2±2.13	0.31±0.04	512.14±48.6
10	H	OH	H	H	OH	OCH_3	3.44±0.41	0.15±0.03	0.41±0.02
11	OCH_3	OCH_3	OCH_3	H	OCH_3	H	0.25±0.02	0.36±0.03	0.38±0.04
12	OCH_3	OCH_3	OCH_3	OCH_3	OCH_3	OCH_3	2.66±0.27	0.39±0.04	2.31±0.25
13	OCH_3	OCH_3	OCH_3	H	OH	OCH_3	0.28±0.03	15.08±1.81	0.51±0.05
14	H	OCH_3	H	OCH_3	OCH_3	OCH_3	0.47±0.04	0.18±0.02	2.55±0.26
15	H	OCH_3	H	H	OH	OCH_3	0.41±0.03	0.19±0.04	5.13±0.54
16	H	OH	H	OCH_3	OCH_3	OCH_3	110±12.62	218.2±22.21	0.51±0.06

a) The values given are mean of four experiments ± S.E.M., HL-60. *b*) Leukemia carcinoma, MCF-7. *c*) Human breast, HCT-116. *d*) Human colon cancer cell lines.

Table 2. *In Vitro* Cytotoxic Activity (IC_{50} μM) of the Compounds **17**–**19** over HL-60, MCF-7 and HCT-116 Cancer Cell Lines

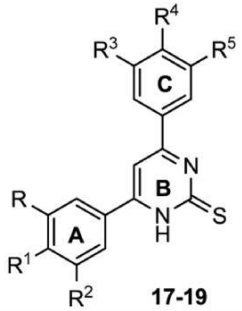

17-19

Comp No.	R	R^1	R^2	R^3	R^4	R^5	(IC_{50} μM)[a]		
							HL-60[b]	MCF-7[c]	HCT-116[d]
17	H	OCH_3	H	OCH_3	OCH_3	OCH_3	4.6±0.39	1.46±0.15	1.65±0.093
18	OCH_3	OCH_3	OCH_3	H	OH	OCH_3	0.36±0.08	0.32±0.07	0.71±0.07
19	OCH_3	OCH_3	OCH_3	OCH_3	OCH_3	OCH_3	7.9±0.81	2.14±0.22	0.56±0.051

a) The values given are mean of four experiments±S.E.M., HL-60. *b*) Leukemia carcinoma, MCF-7. *c*) Human breast, HCT-116. *d*) Human colon cancer cell lines.

Table 3. *In Vitro* Cytotoxic Activity (IC_{50} μM) of the Compounds **20**–**23** over HL-60, MCF-7 and HCT-116 Cancer Cell Lines

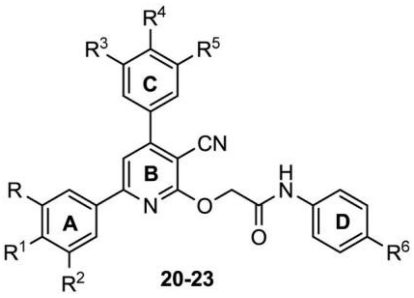

20-23

Comp No.	R	R_1	R_2	R_3	R_4	R_5	R_6	(IC_{50} μM)[a]		
								HL-60[b]	MCF-7[c]	HCT-116[d]
20	OCH_3	OCH_3	OCH	H	OCH_3	H	H	2.58±0.26	2.69±0.33	0.70±0.06
21	OCH_3	OCH_3	OCH_3	H	OCH_3	H	OCH_3	0.09±0.01	0.06±0.007	0.54±0.06
22	OCH_3	OCH_3	OCH_3	OCH_3	OCH_3	OCH_3	H	1.42±0.13	3.8±0.42	3.73±0.42
23	OCH_3	OCH_3	OCH_3	OCH_3	OCH_3	OCH_3	OCH_3	9.24±0.89	1.79±0.18	52.4±5.35

a) The values given are mean of four experiments ± S.E.M., HL-60. *b*) Leukemia carcinoma, MCF-7. *c*) Human breast, HCT-116. *d*) Human colon cancer cell lines.

seven compounds **5**, **12**, **17**, **19**, **20**, **22** and **23** show moderate activity (IC_{50} values ranging from 1.42 to 9.24 μM). Furthermore, compounds **8**, **9** and **16** show weak activity (IC_{50} values ranging from 23 to 110 μM). In respect to MCF-7 cells, ether derivative **21** is equipotent compound to CA-4 (IC_{50}: 0.06 μ M). The following compounds, pyridinthione derivatives **4**, **5**, **7**, **9**, **10**, pyridinone derivatives **11**, **12**, **14**, **15**, pyrimidinthione derivative **18**, and ether derivative **21** show high cytotoxic activity in sub-micromolar concentrations. Regarding HCT cell line, pyidinethione **10** is the most cytotoxic compound (IC_{50}: 0.41 μM) and is 2-fold higher than CA-4. Pyridinthione derivatives **6** and **10**, pyridinone derivatives **11**, **13** and **16** , pyrimidinthione derivatives **18** and **19** and ether derivatives **20** and **21** with sub-micromolar IC_{50} concentration values, show higher activity than control drug (1 μ M). According to the structural modifications of the designed compounds **4**–**23**, a structural activity relationship (SAR) analysis is performed for the three models **A**, **B** and **C** over all three cell lines, as follows.

The structural variations present among pyridine derivatives **4**–**16** (model **A**) are in the core rings, either, pyridinthione or pyridinone, and the different decorations of C-4 and C-6 diaryl groups of core ring. Therefore, model **A** would be further subdivided into 3 sub-models, according to three different kinds of decoration of aryl groups present at C-6 of the pyridine. The first sub-model **A1** includes six compounds **4**–**6** and **11**–**13** and contain the same 3, 4, 5-TMP moiety as C-6 aryl group, a common trait in colchicine and CA-4. Two variations are included in submodel **A1**, sulphur or oxygen, at C-2 of the core and different aryl rings at C-4 of pyridine. Pyridinthione **4** with 4-methoxyphenyl group as C-4 arylation is the most cytotoxic agent within **A1** group and is more potent than CA-4 over HL-60 and MCF-7 cell lines. Furthermore, com-pound **11** that contains 4- methoxyphenyl group as a C -4 aryl of pyridinone is the most cytotoxic agent and is more potent than standard against HCT-116 cell line, indicating that 4 -methoxyphenyl and TMP as a coupled diaryl groups on the core give the best activity in this submodel **A1**. Concerning the presence of oxygen and sulphur, pyridinthiones **4** and **6** have higher cytotoxic activity than pyridinones **11** and **13** against HL-L60 and MCF-7 cell lines. On the other hand, pyridinones **11** and **12** are more cytotoxic than pyridinthiones **4** and **5** against HCT-116 cell line (Table 1). The second sub-model **A2** group includes four pyridine derivatives **7**, **8**, **14** and **15** contain 4 -methoxyphenyl moiety as C- 6 aryl group in pyri-dine. The results show that: pyridinone derivative **14** with 3, 4, 5-TMP group as C -4 arylation with IC_{50} (0.18 and 2.55 μM) is the most cytotoxic agent against MCF-7 and HCT-116 cell lines respectively. Pyridinones **14** and **15** are more cytotoxic than pyridinthiones **7** and **8** against three cell lines, indicating that oxygen is more contributing to cytotoxicity than sulphur in this submodel **A2** (Table 1). The third sub- model **A3** included three pyridine derivatives **9**, **10** and **16** that have the same 4-hydroxyphenyl moiety at C-6 of the pyridine. Pyridinthione **10** that contains 4-hydroxy-3-methoxyphenyl group as C-4 arylation is the most cytotoxic agent of this group against MCF-7, HL-60 and HCT-116 cell lines. Meanwhile, pyridinthione **9** that contains sulphur is more cytotoxic than 2- pyridinone **16** against three cell lines (Table 1). In the light of structural analysis of model, **A** results, it appeared that the cytotoxic activity of pyridine derivatives **4**–**16** correlated to the general skeleton of the decorated diaryl groups, as the presence of TMP and 4-methoxy groups together, either at C- 4 or C-6 of pyridine generated the best cytotoxic activity as in compounds **4**, **11** and **14** (Table 1).

In respect to model **B**, pyrimidinthiones **17** and **18** are more cytotoxic than corresponding pyridinthiones **5** and **7** against both HCT-116 and HL-60 cell lines, while pyridinthiones are more cytotoxic than pyrimidinthiones to MCF-7 cells. Compound **18** with IC_{50}: 0.32 and 0.36 μM over MCF-7 and HL-60 cell lines, respectively is the most potent cytotoxic derivative of the pyrimidines **17**–**19** and the pyridine analogue **6**. The good cytotoxicity profile of compound **18** might have structural similarities with the aryl groups of CA-4 (Table 2). Regarding model **C**, ether derivatives **20** and **21** exhibit a good cytotoxicity higher than compounds **22** and **23**, against HCT-116 and HL60 cells. Also, the obtained data shows that structural extension of pyridinone derivatives **11** and **12** by ether formation result in decreasing the potency of cytotoxic activity, as the ether derivatives **20**, **22** and **23** are less cytotoxic than parent pyridine derivatives **11** and **12**, except in compound **21**

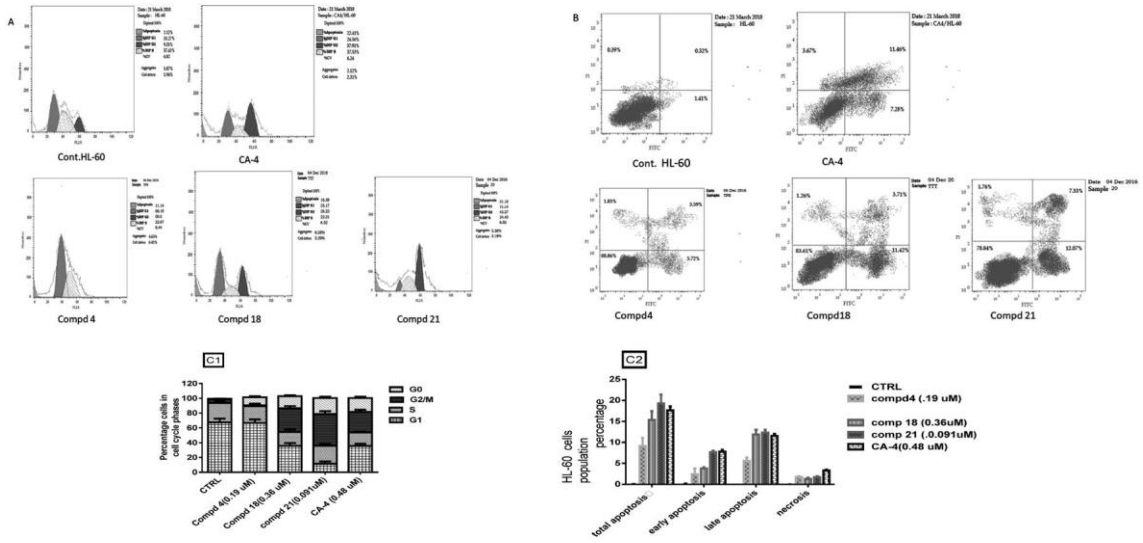

Fig. 3. **A**) Cell Cycle Analysis of Compounds **4** , **18** and **21** on HL-60 Cancer Cells Compared with CA-4 (0.48 μM) as Control Drug at Their IC_{50} (0.19, 0.36 and 0.09 μM, Respectively) for 24h, **B**) Annexin V/PI Staining Analysis for Apoptosis Percentage of Compounds **4**, **18**, **21**, and CA-4 on HL-60 Cancer Cells; **C1**) Statistical Analysis of Cell Cycle Analysis, **C2**) Statistical Analysis of Annexin V/PI Staining Analysis.

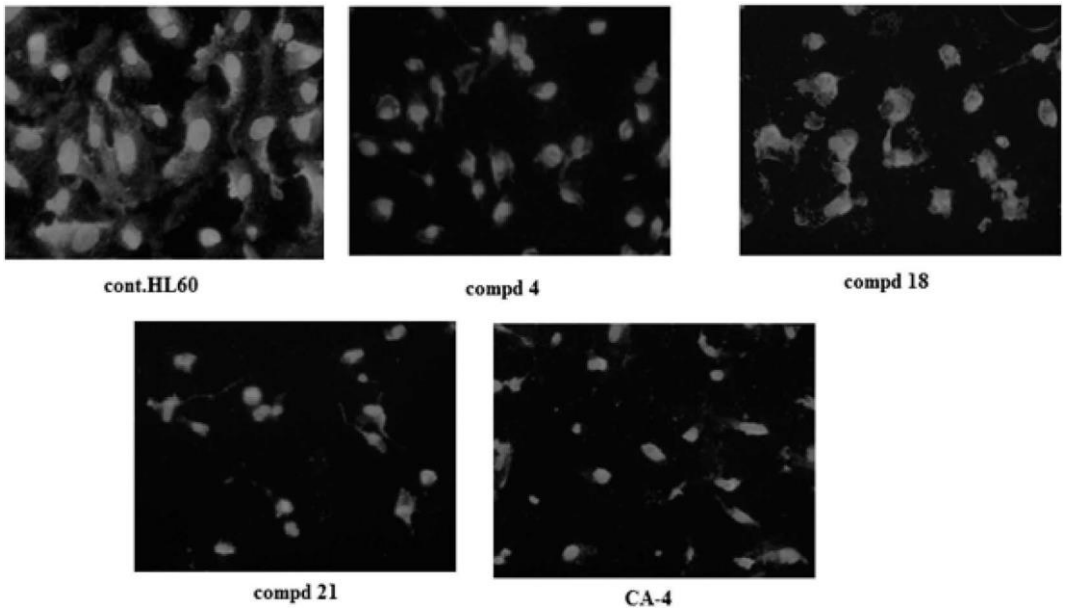

Fig. 4. Fluorescence Intensity (IFU) of Tubulin Localization in HL-60 Cancer Cells for the Effect of Compounds **4**, **18** and **21** Compared with CA-4 (0.48 μM) as Control Drug at Their IC_{50} (0.19, 0.36 and 0.09 μM, Respectively) for 24 h

(Table 3). Ether derivatives **22** and **23** containing TMP group, as coupled C-4 and C-6 diaryl groups, are less cytotoxic than other derivatives. In terms of the effect of *N*-aryl groups on cytotoxicity results, *N*-phenyl acetamide derivative **20** is less cytotoxic than *N*- 4-methoxyphenyl acetamide derivative **21** (Table 3). A brief final conclusion from this results analysis shows that pyridinthiones are more active than pyridinones over HL-60 and MCF-7 cells. This might be due to difference in lipid solubility of sulphur and oxygen. Synthesized pyrimidine derivatives are more active than the corresponding pyridine analogues over HL-60 and HCT-116 cells. Regarding the decoration of the structure of C- 4 and C-6 diaryl groups at the core ring, 4- methoxyphenyl and TMP groups are the most active cytotoxic coupled diaryl groups at C-4 and C-6 of the core. Finally, extension of the structure to increase cytotoxicity is controlled by decoration of the C-4 and C-6 diaryl rings at the core part by either by one or two TMP groups, as in compounds **21** and **23**.

In Vitro DNA-Flow Cytometry Cell Cycle Analysis

Three compounds: pyridinthione derivative **4**, pyrimidinthione **18** and ether derivative **21** over HL-60 cell line (0.19, 0.36 and 0.09 μM, respectively) are selected as potent cytotoxic agents, which represent the three pharmacophoric models **A**, B and **C** to be further studied for their effects on cell cycle progression and induction of apoptosis. The obtained results after treatment of HL-60 cancer cells with compounds **4**, **18** and **21** are shown in Fig. 3A. The results of cell cycle analysis show that a significant change in cell cycle distribution is ob-served compared with untreated HL-60 cells and CA-4.

Pyridine derivative **4** causes a cell cycle at G_1 phase by in-

creasing G_1 phase by 3-fold and decreasing S phase by 2-fold than CA-4. Furthermore, pyrimidine derivative **18** increases the accumulation of cells at G_0, G_1 and G_2/M phase by 1-fold and decreases and S phase by 2-fold compared to CA-4 (Fig. 3C2). In addition, compound **21** increases the G_0 phase and decreases G_1 and S phase about 2-fold compared to CA-4 and increases the accumulation of cells at G_2 /M phase by 2-fold than CA- 4, indicating that of the tested compounds, cause cell cycle block at G_1 and G_2/M phase and hence cell death of HL-60 cells.

Apoptosis Analysis by Annexin V/Propidium Iodide (PI) Staining

To ensure the ability of compounds **4**, **18** and **21** to induce apoptosis, flow cytometry analysis is performed using annex-in-V and PI staining.[46] The results of experiment performed are summarized and presented graphically in (Fig. 3B). After treatment with compounds **4**, **18** and **21** at their IC_{50} concentration, a decrease in the percentage of survived cells is observed. Moreover, a significant increase in the percentage of annexin-V positive cells occurs in compounds **4**, **18** and **21** compared untreated cells and CA-4 indicating that these compounds induced apoptosis in HL-60cells (Fig. 3B). Compound **21** give about 10-fold more potent activity as apoptotic inducer than untreated control cells (Fig. 3C2).

In Vitro Immunofluorescence Localization of Tubulin in HL-60 Cancer Cells

To explore the cell cycle arrest at G_2/M phase induced by the tested compounds **4**, **18** and **21**, immunofluorescence labeling assay for tubulin localization under fluorescence micro-scope is performed after treatment of HL-60 cells with each compound at its IC_{50} for 48 h and then submitted to analysis. The results of assay shows that compound **21** has potent inhibitory effect on cellular tubulin formation higher than CA-4 compared with untreated cells (Fig. 4). Meanwhile compound **18** shows good inhibitory activity but less than compound **21**, while compound **4** shows a moderate degree of tubulin polymerization inhibitory activity as concluded from the inhibition of the fluorescence intensity.

In Vitro β-Tubulin (TUBβ) Polymerization Inhibition Assay

Pyridinthione derivatives **4**, **6**, **11** and **13**, pyrimidinthione **18**, ether derivatives **21** and **23** represent the designed models **A**, **B** and **C** and contain TMP moiety, as C-6 aryl group of the core ring are further investigated for inhibition percentage of β-tubulin polymerization in HL-60 cell line at their IC_{50} *via* enzyme linked immunosorbent assay (ELISA) using human-β-tubulin assay kit.

The inhibitory activity of β-tubulin polymerization is given as the percentage inhibition at IC_{50} concentration of each compound. The results of performed experiment are summarized in (Table 4). Structural analysis of the tested compounds shows that pyrimidine derivative **18** shows higher β-tubulin inhibition percentage than corresponding pyridine derivative **13**. This experimental finding correlates the good

Table 4. Percentage Inhibition of β-Tubulin Polymerization on Human HL-60 Cell Line for the Compounds **4**, **6**, **11**, **13**, **18**, **21**, **23** and **CA-4** at Their IC_{50} (μM)

Comp No.	% Inhibition of tubulin β Polymerization	HL-60[a] IC_{50} (μM)
4	78±1	0.19
6	83±2	0.21
11	71±2	0.25
13	80±2	0.28
18	87±2	0.36
21	94±1	0.09
23	56±3	9.24
CA-4	87±1	0.48

a) The values given are mean of two experiments ± S.E.M. HL-60, leukemia carcinoma cells.

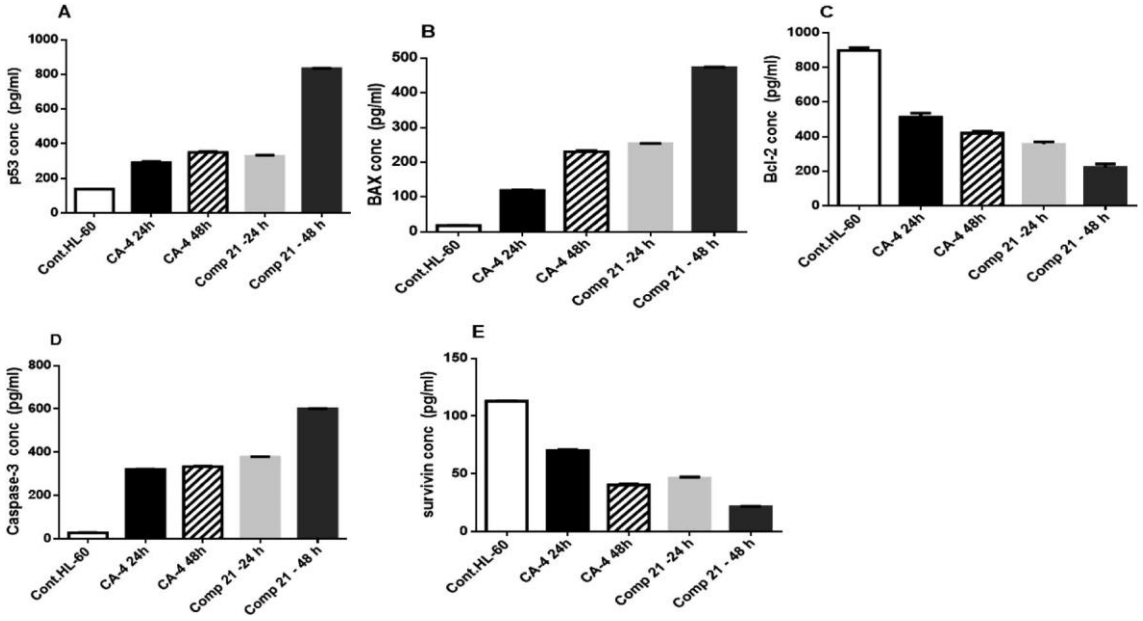

Fig. 5. *In Vitro* Elisa Measurement Showed the Effect of Compound **21** at Its IC_{50} (0.091 μM) for (24, 48 h) on HL-60 Cell Line as Negative Control Compared with CA-4 (0.48 μM) as Control Drug, **A**) Effect on p53, **B**) Effect on Bax Levels, **C**) Effect on Bcl-2, **D**) Effect on Caspase-3 Levels, **E**) Effect on Survivin Levels

Data were expressed as mean (n=4 experiments) ±S.E.M. and statistical comparisons were carried out using one-way ANOVA followed by Tukey multiple comparisons test at p<0.05.

cytotoxic activity of compound **18** to structural similarities of diaryl groups with CA-4. Furthermore, pyridine derivatives **6** and **13** contain sulphur and oxygen, at C -2 of the core ring, show similar inhibition percentage. Ether derivative of pyridine **21** shows higher tubulin inhibition than similar CA-4 and corresponding pyridine derivative **11**. This experimental result supports the aim of the design of model **C**, as the additional group (*N*-aryl acetamide group) might have allowed the structure to possess bitter affinity towards binding sites. Compound **23** shows moderate inhibition percentage parallel to cytotoxic activity results. The results of tubulin inhibition percentage are in agreement of IC_{50} cytotoxicity.

In Vitro ELISA Immunoassay of Apoptosis Mediators

Resistance of tumor cells to apoptosis induction occurred by increasing expression of anti-apoptotic proteins, as Bcl-2 and decreasing pro -apoptotic proteins, as Bax. Both proteins are regulated with p53.[47] Compound **21** is the most potent apoptotic inducer with 12.07% within tested compounds as demonstrated by Anexienn V assay Further investigation of apoptosis inducing activity of compound **21** compared with CA-4 by measuring the concentration of the cancer biomarkers, p53, Bax, Bcl-2, caspase -3 and survivin, is performed using ELISA immunoassay in a time -dependent manner. The obtained results are summarized and graphically represent in (Figs. 5A–E).

Treatment of HL-60 cells to compound **21** in a time-dependent manner result in a significant increasing in the level of p53 by 1- and 2-fold more than CA-4, after 24 and 48 h treatments, respectively (Fig. 5A). Consistent with this up-regulation, the level of Bax increases by 2-fold after 24 and 48 h, compared with CA-4 (Fig. 5B). On the other hand, the level of Bcl-2 decreases by 1- and 2-fold compared with CA-4, for the 24 and 48 h treatments, respectively (Fig. 5C). As compound **21** significantly elevates the Bax/Bcl-2 ratio, therefore, the subsequent step is to measure the level of active caspase-3. Activation of caspase-3 is a final step in mitochondrial induced apoptosis (intrinsic pathway), which result in DNA fragmentation.[48] The results exhibit that the level of caspase-3 increases by 1- and 2-fold, after 24 and 48 h, respectively, compared with CA-4. In conclusion, compound **21** shows a apoptosis inducing activity *via* mitochondrial pathway, by increasing the level of p53, Bax/Bcl-2 ratio and caspase-3 (Fig. 5D). Survivin is an IAP that directly acts on caspase-3 and inhibits its apoptotic actions, even after its activation.[49] Compound **21** decreases the survivin protein level by 1.5- and 2-fold after the 24 and 48 h, respectively, compared with CA-4 (Fig. 5E). The obtained data demonstrate that compound **21** is more potent cytotoxic and apoptotic inducer higher than CA-4. Also, the obtained results rationalized possible mode of cytotoxic activity and high apoptotic inducing activity induced by compound **21** on HL-60 cells.

Conclusion

The biological rationale of the work is the design and construction of a potential antimitotic compounds endowed with pro-apoptotic inducing activity. The design approach is likely to transcend the shortcomings of the existing antimitotic drugs where cancer cells resistance to apoptosis induction by anti-tumor agents will decrease. *In -vitro* cytotoxicity results show a substantial improvement in cytotoxic activity of the synthesized compounds against HL-60, MCF-7 and HCT-116 cell lines, compared with CA-4. The pyridinthione **4** and ether analogue **21** are the most cytotoxic derivatives (IC_{50}: 0.19 and 0.091 μM) against HL -60 cell line, while, in general, eight of compounds: **4**, **6**, **11**, **13**, **14**, **15**, **18** and **21** (IC_{50} values ranging from 0.19 to 0.47 μM) are more potent against HL -60 cell line than CA-4 (0.48 μM). Regarding the cytotoxicity against MCF-7 cell line, ether derivative **21** is an equipotent com-pound to CA-4 (IC_{50}: 0.06 μ M). In addition, the following nine final compounds **4**, **5**, **7**, **9**, **10**, **12**, **14**, **15** and **18** show high cytotoxic activity in sub -micromolar values with a similar cytotoxic potency against both HL-60 and MCF-7 cell lines. In terms of cytotoxic activity against HCT-116 cell line, the most cytotoxic agent towards HCT-116 cells is compound **11** (IC_{50}: 0.38 μM). In addition, nine of the tested compounds **6** , **10**, **11**, **13**, **16**, **18** , **19**, **20** and **21** (sub-micromolar IC_{50}values ranging from 0.18 to 0.71 μM) show higher cytotoxic activity than control drug (1 μM). The obtained results of cell cycle analysis and annexin-V test on HL- 60 cancer cells for the compounds **4**, **18** and **21** show cell cycle arrest at G2/M phase and a potent apo-ptotic activity compared with CA-4. The results of β-tubulin polymerization inhibition percentage of pyridinthione **4**, pyridinone **13**, pyrimidinthione **18** and ether **21**, compared with CA-4, revealed that the tested compounds **18** and **21** possessed excellent β-tubulin inhibition activity. Furthermore, the potent apoptotic inducing activity exhibited by compound **21** higher than CA-4 is rationalized by increasing concentration of p53, Bax/Bcl-2 ratio and caspase-3 proteins and decreasing survivin protein levels. Finally, the small compounds library **4**–**23** represent lead structures for potential antitumor agents against HL -60 cell line and other solid tumor tumors as MCF-7 and HCT-116 cancer cells.

Experimental

Synthesis

General

Solvents and reagents are obtained from Aldrich, Fluca or Merck and are used without further purification unless otherwise indicated. Melting Points are determined on a Griffin apparatus and are uncorrected. The elemental analysis is performed at The Regional Center for Mycology and Biotechnology, Al-Azhar University, Egypt. IR spectra are recorded on a Shimadzu 435 spectrophotometer and Mattson Genesis II FTIR, using KBr discs, Cairo University, and values are rep-resented in cm^{-1}. ^{1}H-NMR spectra were performed Bruker400 MHz&Bruker300 MHz spectrophotometer using TMS as internal standard, chemical shifts (δ) are recorded in ppm on δ scale. ^{13}C-NMR spectra are carried out using Bruker 100 MHz using TMS as internal standard, chemical shifts (δ) are recorded in ppm on δ scale, Micro analytical unit Center, Cairo University, Egypt. Mass spectra are run on Hewlett Packard 5988 spectrometer or shimadzu QP-2010 plus at The Regional Center for Mycology & Biotechnology, Al-Azhar University, Egypt. Progress of the reactions is monitored by TLC using precoated aluminum sheets silica gel (Merck 60 F 254) and is visualized by UV lamp and iodine vapor. The solvent system used in TLC is hexane : ethyl acetate [7 : 3], Mass-II microwave Synthesis work station is used with the following specification, operating frequency 2450 MHz and rated output power range 0–1000 W.

1,3-Diaryl-2-propen-1-ones Ia–c Were Prepared as Reported.[34,35] General Procedure for the Synthesis of 4,6-Diaryl-2-thioxo-1, 2-dihydropyridine-3-carbonitriles (**4**–**10**)

A mixture of the required acetophenones (0.001 mol), the appropriate aromatic aldehydes (0.001 mol), cyanothioacetamide (0.1 g, 0.001 mol) and ammonium acetate (0.62 g, 0.008 mol) in *n*-butanol (10 mL) is irradiated at 150°C for 20 min in the microwave oven. After the reaction mixture is cooled to room temperature, the reaction mixture is diluted with 10 mL diethyl ether and the separated solid is filtered, dried and crystallized from ethanol to afford compounds **4**–**10**.

1,2-Dihydro-6-(3,4,5-trimethoxyphenyl)-4-(4-methoxyphenyl)-2-thioxopyridine-3-carbonitrile (**4**)

Yellow powder, yield: 0.35g (87%), mp: 294–296°C. IR (KBr, cm^{-1}): 3421 (NH), 3066 (CH-aromatic), 2843 (CH-aliphatic), 2222 (CN), 1136 (C=S). ^{1}H -NMR (400 MHz, dimethyl sulfoxide (DMSO)-d_6), δ ppm: 3.73 (s, 3H, OCH_3), 3.85 (s, 3H, OCH_3), 3.88 (s, 6H, 2OCH_3), 6.88 (s, 1H, Ar-H), 7.13 (d, 2H, *J*=7.5 Hz, Ar-H), 7.20 (s, 2H, Ar-H), 7.72 (d, 2H, *J*=7.7 Hz, Ar-H), 12.53 (s, 1H, NH, D_2O exchangeable).^{13}C-NMR (100 MHz, DMSO-d_6), δ ppm: 55.9, 56.2 (2C), 56.7, 97.7, 102.3, 105.8 (2C), 114.6 (2C), 117.4, 128.6, 129.5, 130.5 (2C), 140.4, 153.5 (2C), 155.9, 161.5, 167, 169. *Anal.* Calcd for: $C_{22}H_{20}N_2O_4S$ (408.47): C, 64.69; H, 4.94; N, 6.86. Found: C, 64.93; H, 5.07; N, 7.04.

1,2-Dihydro-4,6-bis (3,4,5-trimethoxyphenyl)-2-thioxopyridine-3-carbonitrile (**5**)

Yellow powder, yield: 0.41 g (87%), mp: 190–192°C. IR (KBr, cm^{-1}): 3408 (NH), 3045 (CH-aromatic), 2837 (CH-aliphatic), 2223 (CN), 1120 (C=S). ^{1}H-NMR (400 MHz, DMSO- d_6), δ ppm: 3.73 (s, 6H, 2OCH_3), 3.75 (s, 6H, 2OCH_3), 3.83 (s, 6H, 2OCH_3), 7.35 (s, 2H, Ar- H), 7.73 (s, 1H, Ar-H), 7.84 (s, 1H, Ar-H), 8.13 (s, 1H, Ar- H), 12.68 (s, 1H, NH, D_2O exchangeable).^{13}C-NMR (100 MHz, DMSO-d_6), δ ppm: 56.5 (4C), 57.6 (2C), 95.3, 105.4 (2C), 107.7, 108.4, 115.5, 117.3, 118 (2C), 127.6, 138.3, 141.5, 149.2, 151.3, 152.9, 153.4, 158.5, 163.2. *Anal.* Calcd for $C_{24}H_{24}N_2O_6S$ (468.52): C, 61.52; H, 5.16; N, 5.98. Found: C, 61.87; H, 5.22; N, 6.05.

1,2-Dihydro-4-(4-hydroxy-3-methoxyphenyl)-6-(3,4,5-trimethoxyphenyl)-2-thioxopyridine-3-carbonitrile (**6**)

Yellow powder, yield: 0.33 g (80%), mp: 296–298°C. IR (KBr, cm^{-1}): 3421–3224 (NH, OH), 3056 (CH-aromatic), 2839 (CH-aliphatic), 2220 (CN), 1139 (C=S). ^{1}H-NMR (400 MHz, DMSO- d_6), δ ppm: 3.73 (s, 3H, OCH_3), 3.85 (s, 3H, OCH_3), 3.88 (s, 6H, 2OCH_3), 4.41 (s, 1H, D_2O exchangeable), 6.89 (s, 1H, Ar- H), 6.94 (d, 1H, *J*=7.3 Hz, Ar-H), 7.19 (s, 2H, Ar- H), 7.23 (d, 2H, *J*=7.1 Hz, Ar-H+H, D_2O exchangeable), 7.32 (s, 1H, Ar-H). ^{13}C- NMR (100 MHz, DMSO-d_6), δ ppm: 56.7, 60.1 (2C), 60.6, 100, 102.1, 105.8 (2C), 116, 117.3, 122.5, 125.2, 133, 138.7, 141.5, 148, 149.5, 153.5 (2C), 163.2, 167.7, 169.2. *Anal.* Calcd for $C_{22}H_{20}N_2O_5S$ (424.47): C, 62.25; H, 4.75; N, 6.60. Found: C, 62.39; H, 4.81; N, 6.53.

1,2-Dihydro-4-(3,4,5-trimethoxyphenyl)-6-(4-methoxyphenyl)-2-thioxopyridine-3-carbonitrile (**7**)

Orange powder, yield: 0.35 g (85%), mp: 293–295°C. IR (KBr, cm^{-1}): 3425 (NH), 3068 (CH-aromatic), 2843 (CH-aliphatic), 2197 (CN), 1127 (C=S). ^{1}H-NMR (400 MHz, DMSO-d_6), δ ppm: 2.51 (s, 1H, NH, D_2O exchangeable), 3.71 (s, 3H, OCH_3), 3.79 (s, 3H, OCH_3), 3.83 (s, 6H, 2OCH_3), 6.57 (s, 1H, Ar-H), 6.87 (s, 2H, Ar-H), 6.95 (d, 2H, *J*=7.8 Hz, Ar-H), 7.97 (d, 2H, *J*=7.6 Hz, Ar-H). ^{13}C-NMR (100 MHz, DMSO-d_6), δ ppm: 56.0, 56.6 (2C), 60.6, 105.5, 106.5, 114.8 (2C), 117.4 (2C), 125.5, 130 (2C), 131.8, 139.6, 152.1, 153.3 (2C), 160.1, 162.3, 162.6, 169.7. *Anal.* Calcd for $C_{22}H_{20}N_2O_4S$ (408.47): C, 64.69; H, 4.94; N, 6.86. Found: C, 64.98; H, 5.01; N, 6.98.

1,2-Dihydro - 4 - (4 -hydroxy-3-methoxyphenyl) - 6 - (4 -methoxyphenyl)-2-thioxopyridine-3-carbonitrile (**8**)

Yellow powder, yield: 0.29 g (83%), mp: 295–297°C. IR (KBr, cm^{-1}): 3471–3360 (NH, OH), 3077 (CH -aromatic), 2833 (CH -aliphatic), 2202 (CN), 1128 (C=S). ^{1}H-NMR (300 MHz, DMSO-d_6), δ ppm: 3.63 (s, 6H, 2OCH_3), 6.12 (d, 2H, *J*=7.1 Hz, Ar-H), 6.91 (brs, 2H, D_2O exchangeable), 7.17 (d, 2H, *J*=7.2 Hz, Ar-H), 7.44 (s, 2H, Ar-H), 7.67 (d, 2H, *J*=6.9 Hz, Ar-H).^{13}C-NMR (100 MHz, DMSO-d_6), δ ppm: 56, 56.3, 98.2, 105.4 (2C), 113, 114.8, 116, 117.7, 122.2, 124.8, 127.3, 129.9 (2C), 148, 149.5, 150.8, 160.1, 162.1, 162.8. *Anal.* Calcd for $C_{20}H_{16}N_2O_3S$ (364.42): C, 65.92; H, 4.43; N, 7.69. Found: C, 66.17; H, 4.51; N, 7.94.

1,2-Dihydro-6-(4-hydroxyphenyl)-4-(3,4,5-trimethoxyphenyl)-2-thioxopyridine-3-carbonitrile (**9**)

Yellow powder, Yield: 0.34 g (86%), mp: 260–262°C. IR (KBr, cm^{-1}): 3406–3231 (NH, OH), 3060 (CH-aromatic), 2837 (CH-aliphatic), 2223 (CN), 1170 (C=S). ^{1}H-NMR (400 MHz, DMSO- d_6), δ ppm: 3.77 (s, 3H, OCH_3), 3.83 (s, 6H, 2OCH_3), 6.78 (s, 1H, Ar-H), 6.88 (d, 2H, *J*=7.6 Hz, Ar-H), 7.04 (s, 1H, Ar-H), 7.36 (s, 1H, Ar-H), 7.79 (d, 2H, *J*=7.4 Hz, Ar-H), 10.23 (s, 1H, OH, D_2O exchangeable), 12.47 (s, 1H, NH, D_2O exchangeable). ^{13}C-NMR (100 MHz, DMSO-d_6), δ ppm: 56.5 (2C), 56.6, 105.5, 106.5, 108.4 (2C), 116.2 (2C), 117.3, 127.6 (2C), 130.1, 131.9, 139.5, 141.5, 151.3, 153.4 (2C), 160.7, 163.2. *Anal.* Calcd for $C_{21}H_{18}N_2O_4S$ (394.44): C, 63.94; H, 4.60; N, 7.10. Found: C, 64.17; H, 4.68; N, 7.26.

1,2-Dihydro - 4 - (4 -hydroxy-3-methoxyphenyl) - 6 - (4 -hydroxyphenyl)-2-thioxopyridine-3-carbonitrile (**10**)

Yellow powder, yield: 0.28 g (80%), mp: >300°C. IR (KBr, cm^{-1}): 3421–3319 (NH, OH), 3021 (CH-aromatic), 2835 (CH-aliphatic), 2218 (CN), 1120 (C=S). ^{1}H-NMR (400 MHz, DMSO -d_6), δ ppm: 3.86 (s, 3H, OCH_3), 6.71–6.72 (m, 3H, Ar-H+ OH, D_2O exchangeable), 6.89–6.91 (d, 2H, *J*=7.4 Hz, Ar-H), 7.23 (d, 1H, *J*=7.7 Hz, Ar-H), 7.32 (d, 1H, *J*=7.6 Hz, Ar-H), 7.77 (s, 1H, Ar-H), 7.84 (s, 2H, Ar-H), 9.88 (s, 1H, OH, D_2O exchangeable), 12.03 (s, 1H, NH, D_2O exchangeable). ^{13}C-NMR (100 MHz, DMSO-d_6), δ ppm: 56.3, 96.4, 104.9 (2C), 113, 116, 116.2, 117.9, 122.2, 123.2, 127.4 (2C), 130, 148, 149.5, 151.2, 160, 160.9, 162.8. *Anal.* Calcd for $C_{19}H_{14}N_2O_3S$ (350.39): C, 65.13; H, 4.03; N, 7.99. Found: C, 65.41; H, 3.97; N, 8.21.

General Procedure for the Synthesis of 4,6-Diaryl-2-oxo-1,2-dihydropyridine-3-carbonitriles (**11**–**16**)

A mixture of the appropriate acetophenone (0.001 mol), the aromatic aldehydes (0.001 mol), ethyl cyanoacetate (0.15 g, 0.001 mol), and ammonium acetate (0.62 g, 0.008 mol) in *n*-butanol (10 mL) is stirred for 5 min at room temperature and then irradiates at 150°C for 10 min in the microwave oven. After cooling to room temperature, the reaction mixture is diluted with pet. Ether (20 mL). The formed solid is filtered, dried and crystallized from ethanol to give pyridine-3-carbonitrile derivatives **11**–**16.**

1,2-Dihydro-6-(3,4,5-trimethoxyphenyl)-4-(4-methoxyphenyl)-2-oxopyridine-3-carbonitrile (**11**)

Yellow powder, yield: 0.33 g (86%), mp: 286–288°C. IR (KBr, cm^{-1}): 3448 (NH), 3050 (CH-aromatic), 2843 (CH-ali-

phatic), 2214 (CN), 1635 (C=O). ^{1}H-NMR (400 MHz, DMSO-d_6), δ ppm: 3.73 (s, 3H, OCH_3), 3.84 (s, 3H, OCH_3), 3.88 (s, 6H, $2OCH_3$), 6.87 (s, 1H, ArH), 7.12 (d, 2H, *J*=7.6 Hz, Ar-H), 7.20 (s, 2H, Ar-H), 7.72 (d, 2H, *J*=7.3 Hz, Ar-H), 12.63 (s, 1H, NH, D_2O exchangeable). ^{13}C-NMR (100 MHz, DMSO-d_6), δ ppm: 55.9, 56.7 (2C), 60.6, 105.8, 106, 114.6 (2C), 117.4 (2C), 127.7, 128.6, 130.5 (2C), 133.7, 140.4, 151, 153.5 (2C), 159.9, 161.5, 162.5. MS: *m*/*z* (%) 392M^+ (100), 377 (M-15) (47.87), 349 (M-43) (28.27). *Anal.* Calcd for $C_{22}H_{20}N_2O_5$ (392.4): C, 67.34; H, 5.14; N, 7.14. Found: C, 67.45; H, 5.18; N, 7.04.

1,2-Dihydro-4,6-bis (3,4,5-trimethoxyphenyl)-2-oxopyridine-3-carbonitrile (**12**)

Yellow powder, yield: 0.38 g (85%), mp: 286–288°C. IR (KBr, cm^{-1}): 3448 (NH), 3046 (CH-aromatic), 2839 (CH-aliphatic), 2223 (CN), 1650 (C=O). ^{1}H-NMR (400 MHz, DMSO-d_6) δ ppm: 3.73 (s, 3H, OCH_3), 3.75 (s, 3H, OCH_3), 3.86 (s, 6H, $4OCH_3$), 3.88 (s, 6H, $4OCH_3$), 6.97 (s, 1H, Ar-H), 7.04 (s, 2H, Ar-H), 7.20 (s, 2H, Ar-H), 12.69 (s, 1H, NH, D_2O exchangeable). ^{13}C-NMR (100 MHz, DMSO-d_6), δ ppm: 56.7 (4C), 60.6 (2C), 103.7, 105.9 (2C), 106.6 (2C), 115.3, 117.3, 125.3, 127.7, 131.8, 139.6, 140.4, 151.1, 153.3, 153.5, 157.4, 160.3, 162.4. *Anal.* Calcd for $C_{24}H_{24}N_2O_7$ (452.46): C, 63.71; H, 5.35; N, 6.19. Found: C, 63.95; H, 5.43; N, 6.42.

1,2-Dihydro-4-(4-hydroxy-3-methoxyphenyl)-6-(3,4,5-trimethoxyphenyl)-2-oxopyridine-3-carbonitrile (**13**)

Orange powder, yield: 0.37 g (91%), mp: 291–293°C. IR (KBr, cm^{-1}): 3446–3226 (NH, OH), 3076 (CH-aromatic), 2843 (CH-aliphatic), 2218 (CN), 1651 (C=O). ^{1}H-NMR (400 MHz, DMSO-d_6), δ ppm: 3.72 (s, 3H, OCH_3), 3.85 (s, 3H, OCH_3), 3.87 (s, 6H, $2OCH_3$), 6.39 (s, 1H, D_2O exchangeable), 6.87 (s, 1H, Ar-H), 6.96 (d, 1H, *J*=7.4 Hz, Ar-H), 7.18 (d, 1H, *J*=7.3 Hz, Ar-H), 7.22 (s, 2H, *J*=7.4 Hz, Ar-H), 7.29 (s, 2H, Ar-H). ^{13}C-NMR (100 MHz, DMSO-d_6), δ ppm: 56.2, 56.6 (2C), 60.6, 96.3, 105.6, 105.7, 113.1 (2C), 116, 118.4, 122.1, 127.6, 129.5, 140, 148, 149.5, 152.4, 153.4 (2C), 159.2, 164.8. *Anal.* Calcd for $C_{22}H_{20}N_2O_6$ (408.4): C, 64.70; H, 4.94; N, 6.86. Found: C, 64.96; H, 5.01; N, 7.03.

1, 2 - D i h yd r o - 4 - (3, 4, 5 - t r i m e t h ox y p h e n yl) - 6 - (4 - methoxyphenyl)-2-oxopyridine-3-carbonitrile (**14**)

Yellow powder, yield: 0.32 g (85%), mp: >300°C. IR (KBr, cm^{-1}): 3443 (NH), 3032 (CH-aromatic), 2841 (CH-aliphatic), 2216 (CN), 1663 (C=O). ^{1}H-NMR (300 MHz, DMSO-d_6), δ ppm: 3.74 (s, 3H, OCH_3), 3.84 (s, 6H, $2OCH_3$), 3.86 (s, 3H, OCH_3), 4.31 (s, 1H, D_2O exchangeable), 6.83 (s, 2H, Ar-H), 7.05 (s, 2H, Ar-H), 6.08 (d, 2H, *J*=7.3 Hz, Ar-H), 7.90 (d, 2H, *J*=7.4 Hz, Ar-H), 12.60 (s, 1H, NH, D_2O exchangeable). ^{13}C-NMR (100 MHz, DMSO-d_6), δ ppm: 56, 56.6 (2C), 60.6, 105.6, 106.5, 114.8 (2C), 117.4 (2C), 124.8, 130 (2C), 131.8, 139.6, 147.7, 151.3, 153.3 (2C), 160, 162.2, 162.6. *Anal.* Calcd for $C_{22}H_{20}N_2O_5$ (392.4): C, 67.34; H, 5.14; N, 7.14. Found: C, 67.52; H, 5.09; N, 7.28.

1,2-Dihydro - 4 - (4 -hydroxy-3-methoxyphenyl) - 6 - (4 - methoxyphenyl)-2-oxopyridine-3-carbonitrile (**15**)

Yellow powder, yield: 0.3 g (88%), mp: >300°C. IR (KBr, cm^{-1}): 3435–3143 (NH, OH) 3071 (CH-aromatic), 2838 (CH-aliphatic), 2215 (CN), 1653 (C=O). ^{1}H-NMR (300 MHz, DMSO-d_6) δ ppm: 3.83 (s, 3H, OCH_3), 3.85 (s, 3H, OCH_3), 6.76 (s, 1H, Ar-H), 6.92 (d, 2H, *J*=7.6 Hz, Ar-H), 7.05 (d, 2H, *J*=7.5 Hz, Ar-H), 7.23 (d, 1H, *J*=7.2 Hz, Ar-H), 7.32 (s, 1H, Ar-H), 7.87 (d, 1H, *J*=7.9 Hz, Ar-H), 9.65 (s, 1H, D_2O exchangeable), 12.48 (s, 1H, D_2O exchangeable). ^{13}C-NMR (100 MHz, DMSO-d_6), δ ppm: 56, 56.3, 97, 105.4, 113, 114.8 (2C), 116, 117.7, 122.2, 124.8, 127.3, 129.9 (2C), 148, 147.5, 150.8, 160.1, 162.1, 162.8. *Anal.* Calcd for $C_{20}H_{16}N_2O_4$ (348.35): C, 68.96; H, 4.63; N, 8.04. Found: C, 68.89; H, 4.68; N, 8.21.

1,2-Dihydro-6-(4-hydroxyphenyl)-4-(3,4,5-trimethoxyphenyl)-2-oxopyridine-3-carbonitrile (**16**)

Yellow powder, yield: 0.33 g (89%), mp: 298–300°C. IR (KBr, cm^{-1}): 3421–3228 (NH, OH) 3042 (CH-aromatic), 2835 (CH-aliphatic), 2210 (CN), 1631 (C=O). ^{1}H-NMR (400 MHz, DMSO-d_6), δ ppm: 3.73 (s, 3H, $3OCH_3$), 3.85 (s, 6H, $2OCH_3$), 5.85 (s, 2H, D_2O exchangeable), 6.75 (s, 1H, Ar-H), 6.86 (d, 2H, *J*=7.7 Hz, Ar-H), 6.97 (s, 2H, Ar-H), 7.83 (d, 2H, *J*=7.5 Hz, Ar-H). ^{13}C-NMR (100 MHz, DMSO-d_6), δ ppm: 56.6 (2C), 60.6, 104.6, 106.4 (2C), 116.1 (2C), 118.7, 123.4, 125.1, 129.7, 132.8, 139.1 (2C), 153.2 (2C), 154, 158.5, 160.9, 165.7. *Anal.* Calcd for $C_{21}H_{18}N_2O_5$ (378.38): C, 66.66; H, 4.79; N, 7.40. Found: C, 66.90; H, 4.88; N, 7.57.

General Procedure for the Synthesis of 4,6-Diaryl-3,4-dihydropyrimidine-2-(1*H*) thione (**17**–**19**)

The corresponding chalcone **1**–**3** (0.003 mol) and thiourea (0.03 mol) are added successively to a solution of sodium ethoxide (0.003 mol) in absolute ethanol (15 mL). The reaction mixture is irradiated at 100°C for 10 min. The solvent is evaporated and the residue is dissolved in water (10 mL). The alkaline solution is acidified with acetic acid (10 mL) and the precipitated solid is separated by filtration and crystallized from ethanol to produce compounds **17**–**19.**

3,4-Dihydro-4-(3,4,5-trimethoxyphenyl)-6-(4-methoxyphenyl) pyrimidine-2-(1*H*) thione (**17**).[15] 3,4-Dihydro-6-(3,4,5-trimethoxy phenyl) - 4 - (4 -hydroxy-3 -methoxy phenyl) - pyrimidine-2-(*1H*) thione (**18**)

Yellow powder, Yield: 0.81 g (71%), mp: 223–225°C. IR (KBr, cm^{-1}): 3421–3215 (NH, OH), 3030 (CH-aromatic), 2835 (CH-aliphatic), 1120 (C=S). ^{1}H-NMR (400 MHz, DMSO -d_6), δ ppm: 3.77 (s, 3H, OCH_3), 3.80 (s, 3H, OCH_3), 3.82 (s, 6H, $2OCH_3$), 4.32 (s, 1H, D_2O exchangeable), 5.04 (d, 1H, CH pyrimidine), 5.41 (d, 1H, CH pyrimidine), 6.52 (s, 1H, Ar-H), 6.81 (s, 2H, Ar-H), 6.96 (d, 1H, *J*=7.7 Hz, Ar-H), 7.24 (d,1H, *J*=7.5 Hz, Ar-H), 9.02 (s, 1H, D_2O exchangeable), 9.83 (s, 1H, D_2O exchangeable). ^{13}C-NMR (100 MHz, DMSO-d_6), δ ppm: 55.4, 55.6 (2C), 56.2, 103.2 (2C), 114.5 (2C), 123.7, 129.2 (2C), 134.4, 136.5, 136.7, 138.2, 138.4, 153.1 (2C), 159.3 175.15. *Anal.* Calcd for $C_{20}H_{22}N_2O_5S$ (402.12): C, 59.69; H, 5.51; N, 6.96. Found: C, 59.79; H, 5.68; N, 6.84.

4,6-Bis (3,4,5-trimethoxyphenyl) pyrimidine-2-(1*H*) thione (**19**)

Yellow powder, yield: 0.93 g (70%) mp: 205–207°C. IR (KBr, cm^{-1}): 3423 (NH), 3045 (CH-aromatic), 2835 (CH-aliphatic), 1120 (C=S). ^{1}H-NMR (400 MHz, DMSO- d_6), δ ppm: 3.76 (s, 6H, $2OCH_3$), 3.92 (s, 12H, $4OCH_3$), 7.42 (s, 2H, Ar-H), 7.50 (s, 2H, Ar-H), 7.74 (s, 1H, CH pyrimidine), 13.52 (s, 1H, D_2O exchangeable). ^{13}C-NMR (100 MHz, DMSO -d_6), δ ppm: 56.7 (2C), 56.8 (2C), 58.7, 60.7, 104.9 (2C), 106.1, 106.5, 108.1 (2C), 126.3, 128.4, 138.6, 141.4, 141.9, 153.5 (2C), 165.4, 175.8, 181. *Anal.* Calcd for $C_{22}H_{24}N_2O_6S$ (444.5): C, 59.45; H, 5.44; N, 6.30. Found: C, 59.39; H, 5.50; N, 6.49.

2-Chloro-*N*-aryl-acetamides Were Prepared as Reported.[50] General Procedure for the Synthesis of 2-(3-cyano-4,6-diaryl-pyridin-2-yloxy)-*N*-aryl Acetamide (**20**–**23**)

To a solution of the corresponding 3-cyano-2-pyridinones **11** or **12** (0.001 mol) in ethanol (10 mL) containing anhydrous

potassium carbonate (0.56 g, 0.004 mol), the appropriate 2-chloroacetamide derivatives (0.001 mol) are added. The reaction mixture is stirred with irradiation in the microwave oven at 100°C for 15 min, the reaction mixture is cooled and poured onto crushed ice and the separated solid is filtered, washed with water, dried and crystallized from ethanol to furnish compounds **20**–**23**.

2-(3-Cyano-6-(3,4,5-trimethoxyphenyl)-4-(4-methoxyphenyl) pyridin-2-yloxy)-*N*-phenyl Acetamide (**20**)

Yellowish green powder, yield: 0.37 g (72%), mp: 174–176°C. IR (KBr, cm^{-1}): 3444 (NH), 3072 (CH -aromatic), 2830 (CH -aliphatic), 2221 (CN), 1687 (C=O). ^{1}H- NMR (400 MHz, DMSO-d_6), δ ppm: 3.67 (s, 9H, 3OCH_3), 3.87 (s, 3H, OCH_3), 5.18 (s, 2H, CH_2), 7.06–7.08 (m, 2H, Ar-H), 7.17–7.19 (d, 2H, *J*=7.1 Hz, Ar-H), 7.29–7.33 (m, 2H, Ar-H),7.44 (s, 1H, Ar-H), 7.59–7.61 (d, 2H, *J*=7.9 Hz, Ar-H), 7.75 (d, 2H, *J*=7.4 Hz, Ar-H), 7.88 (s, 1H, Ar-H), 10.36 (s, 1H, NH, D_2O exchangeable). ^{13}C-NMR (100 MHz, DMSO-d_6), δ ppm: 55.6, 56.4, 56.7, 60.6, 92.5, 105.4 (2C), 114.4, 114.6, 116 (2C), 121 (2C), 127.8, 128.4, 131.6, 131.8, 132.3 (2C), 140.3, 153.3, 153.5, 153.6, 155.8 (2C), 156.6, 156.9, 161.3, 163.7, 166.2. *Anal.* Calcd for $C_{30}H_{27}N_3O_6$ (525.5), Calcd: C, 68.56; H, 5.18; N, 8.00. Found: C, 68.79; H, 5.26; N, 7.89.

2-(3-Cyano-6-(3,4,5-trimethoxyphenyl)-4-(4-methoxyphenyl) pyridin-2-yl oxy)-*N*-(4-methoxyphenyl) acetamide (**21**)

Greyish powder, Yield: 0.38 g (69%) mp: 170–172°C. IR (KBr, cm^{-1}): 3257 (NH), 3021 (CH-aromatic), 2837 (CH-aliphatic), 2220 (CN), 1672 (C=O). ^{1}H-NMR (400 MHz, DMSO-d_6), δ ppm: 3.68 (s, 3H, OCH_3), 3.70 (s, 6H, 2OCH_3), 3.72 (s, 3H, OCH_3), 3.87 (s, 3H, OCH_3), 5.14 (s, 2H, CH_2), 6.88 (d, 2H, *J*=7.8 Hz, Ar-H), 7.16–7.18 (m, 2H, Ar-H), 7.45–7.51 (m, 4H, Ar-H), 7.75 (d, 2H, *J*=7.4 Hz, Ar-H), 7.88 (s, 1H, Ar-H), 10.21 (s, 1H, NH, D_2O exchangeable). ^{13}C-NMR (100 MHz, DMSO-d_6), δ ppm: 55.6, 55.9, 56.4 (2C), 60.6, 92, 105.3 (2C), 114.3, 114.8, 116.1 (2C), 121, 121.1, 128.4 (2C), 130.6, 130.7 (2C), 132.3 (2C), 140.3, 153.4, 153.6, 155.8 (2C), 156.6, 156.9, 161.3, 163.7, 166.2. *Anal.* Calcd for $C_{31}H_{29}N_3O_7$ (555.58): C, 67.02; H, 5.26; N, 7.56. Found: C, 67.23; H, 5.40; N, 7.68.

2-(3-Cyano-4,6-bis(3,4,5-trimethoxyphenyl)pyridin-2-yloxy)-*N*-phenyl Acetamide (**22**)

Green crystals, yield: 0.38 g (65%) mp: 168–170°C. IR (KBr, cm^{-1}): 3257 (NH), 3012 (CH-aromatic), 2837 (CH-aliphatic), 2220 (CN), 1672 (C=O). ^{1}H-NMR (400 MHz, DMSO-d_6), δ ppm: 3.67 (s, 6H, 2OCH_3), 3.71 (s, 3H, OCH_3), 3.75 (s, 3H, OCH_3), 3.76 (s, 3H, OCH_3), 3.89 (s, 3H, OCH_3), 5.19 (s, 2H, CH_2), 7.04–7.08 (m, 3H, Ar-H), 7.29–7.33 (m, 2H, Ar-H), 7.44 (s, 2H, Ar-H), 7.59–7.61 (d, 2H, *J*=7.5 Hz, Ar-H), 7.94 (s, 1H, Ar-H), 10.37 (s, 1H, D_2O exchangeable). ^{13}C- NMR (100 MHz, DMSO-d_6), δ ppm: 56.3 (2C), 56.7 (2C), 60.6 (2C), 92.4, 105.4 (2C), 107, 114.7 (2C), 116, 119.5, 119.8, 123.9 (2C), 129.3, 130.9, 131.5 (2C), 132.3, 139.2, 139.4, 140.3, 153.3, 153.6, 156.9 (2C), 157.1, 163.6, 166.7. *Anal.* Calcd for $C_{32}H_{31}N_3O_8$ (585.6): C, 65.63; H, 5.34; N, 7.18. Found: C, 65.85; H, 5.30; N, 7.29.

2-(3-Cyano-4,6-bis(3,4,5-trimethoxyphenyl)pyridin-2-yloxy)-*N*-(4-methoxyphenyl) Acetamide (**23**)

Gray powder, Yield: 0.43 g (71%), m.p: 156–158°C. IR (KBr, cm^{-1}): 3257 (NH), 3037 (CH-aromatic), 2837 (CH-aliphatic), 2220 (CN), 1672 (C=O). ^{1}H-NMR (400 MHz, DMSO-d_6), δ ppm: 3.70 (s, 3H, OCH_3), 3.73 (s, 6H, 2OCH_3), 3.75 (s, 3H, OCH_3), 3.86 (s, 6H, 2OCH_3), 3.89 (s, 3H, OCH_3), 4.66 (s, 2H, CH_2), 6.72 (s, 1H, ArH), 6.89–6.91 (m, 3H, ArH), 7.04 (s, 1H, ArH), 7.08 (s, 2H, ArH), 7.46 (d, 2H, *J*=7.5 Hz, Ar-H), 10.14 (s, 1H, D_2O exchangeable). ^{13}C-NMR (100 MHz, DMSO-d_6), δ ppm: 55.6, 56.4 (2C), 56.7, 60.6 (2C), 66, 92.5, 105.4, 105.9, 106.6 (2C), 114.4 (2C), 116 (2C), 117.3, 121.1 (2C), 131.6, 132.3 (2C), 139.4, 139.6, 140.3 (2C), 166.2. MS: *m*/*z* (%) 615 M^+ (5.6). *Anal.* Calcd for $C_{33}H_{33}N_3O_9$ (615.63): C, 64.38; H, 5.40; N, 6.83. Found: C, 64.52; H, 5.47; N, 6.96.

Biological Evaluation

In Vitro Cytotoxic Activity of Compounds **4**–**23** over HL-60, MCF-7 and HCT-116 Cancer Cell Lines.

Materials

The human leukemia cell line (HL-60), breast adenocarcinoma cell line (MCF-7) and colon cancer cell line (HCT-116) were obtained as a gift from NCI, MD, U.S.A. All chemicals and solvents were purchased from Sigma-Aldrich (U.S.A.). CA-4 was purchased from Sigma-Aldrich.

Methodology

The cells are grown on RPMI-1640 medium supplemented with 10% inactivated fetal calf serum and 50 μg/mL gentamycin. The cells are maintained at 37°C in a humidified atmosphere with 5% CO_2 and are subcultured two to three times a week. For antitumor assays, the tumor cell lines are suspended in medium at concentration 5×10^4 cell/well in Corning® 96-well tissue culture plates, then incubated for 24h. The tested molecules **4**–**23** are then added into 96 -well plates (six replicates) to achieve eight concentrations for each compound. Six vehicle controls with media or 0.5% dimethyl sulfoxide (DMSO) are run for each 96 well plate as a control. After incubating for 24 h, the numbers of viable cells are determined by the MTT test.[43] Briefly, the media is removed from the 96 well plate and replaced with 100 μL of fresh culture RPMI 1640 medium without phenol red then 10 μL of the 12 mM MTT stock solution (5 mg of MTT in 1 mL of phosphate buffered saline (PBS)) to each well including the un-treated controls. The 96 well plates are then incubated at 37°C and 5% CO_2 for 4h. An 85 μL aliquot of the media is removed from the wells, and 50 μL of DMSO is added to each well and mixed thoroughly with the pipette and incubated at 37°C for 10 min. Then, the optical density is measured at 590 nm with the microplate reader (Sun Rise, TECAN, Inc., U.S.A.) to determine the number of viable cells and the percentage of viability is calculated as [1−(ODt/ODc)] ×100% where ODt is the mean optical density of wells treated with the tested sample and ODc is the mean optical density of untreated cells. The relation between surviving cells and drug concentration is plotted to get the survival curve of each tumor cell line after treatment with the specified compound. The IC_{50}, the concentration required to cause toxic effects in 50% of intact cells, is estimated from graphic plots of the dose response curve for each conc. using Graph pad Prism software. Each concentration is repeated four times and the mean of the results.

In Vitro DNA-Flow Cytometry Cell Cycle Analysis. Cell Culture and Lysate Collection

HL-60 cells are cultured in RPMIþ10% +5% FBS penicillin/streptomycin and are incubated at humidity 5% CO_2 and maintained at 37°C. HL-60 cells are treated with the IC_{50} concentration of **4**, **18** and **21** (0.19, 0.36 and 0.091 μM) and CA-4 (0.48 μM), HL-60 cells are cultured as a monolayer in T-25 flasks and are seeded to attain 30% confluency prior to treatment. The main 100 mM stock dissolved in DMSO is diluted with cell culture medium in order to reach the previously de-

termined IC_{50} concentration of each of the three preparations. After 24h of treatment with **4**, **18** and **21**, HL-60 cells are collected *via* trypsinization and centrifuged at 10000 rpm. The pellet is then rinsed with PBS and lysed in RIPA lysis buffer at 4°C for 45 min, then centrifuged at 14000 rpm for 20 min to remove the cellular debris. Cell lysates are then collected and stored at 80°C for later protein determination and immuno-assays. Cell lysates stained by propidium iodide and analyzed by flow cytometry using FACS caliber (Becton Dickinson). The experiment is repeated four times and the mean of the results are statistically analyzed. The cell cycle distributions are calculated using Cell-Quest software (Becton Dickinson, San Jose, CA, U.S.A.).

Apoptosis Analysis by Annexin V/PI Staining

HL-60 cells are seeded into each well of a 6-well plate and treated with compounds **4**, **18**, **21** and **CA- 4** at the IC_{50} concentration for 24h. Staining was performed using FITC Annexin V Apoptosis Detection Kit II, BD Pharmingen (BD Biosciences, U.S.A.) according to the manufacturer protocol.[19] Briefly, cells were washed with PBS at least three times, re-suspended in 1× binding buffer, and FITC-conjugated an-nexin V and PI was added for 15 min in the dark. Samples were analyzed by a LSR-II flow cytometer (Becton-Dickinson, San Jose, CA, U.S.A.).

In Vitro Immunofluorescence Localization of Tubulin in HL-60 Cancer Cells

Slides of fixed HL- 60 cells after treatment with the tested compounds **4**, **18** and **21** are rinsed in three changes of PBS. Antigen retrieval step, by which the availability of the antigen for interaction with a specific antibody is maximized. Then, slides are directly transferred to pre-cooled antigen retrieval solution placed at 4°C for 5 min. Non-specific binding of the antibody is prevented by incubating the slides in blocking solution at 37°C for 30 min. Slides are then incubated for 30 min at 37°C with rabbit anti-human tubulin antibody (1 : 500) diluted with blocking solution. Excess antiserum was rinsed from the slide by immersing in cold buffer for two changes of 5–10 min each. Slides are then incubated at 37°C with goat FITC anti-rabbit immuno-globulin G (IgG) (1 : 2500) diluted with blocking solution. The slides are rinsed in the enzyme substrate till the color developed. Images are visualized using a fluorescence microscope (Axiostar Plus, Zeiss, Goettingen, Germany) equipped with image analyzer and digital camera (Power Shot A20, Canon, U.S.A.).

In Vitro β-Tubulin Polymerization. Inhibition Assay

Materials

Enzyme linked immunosorbent assay (ELISA) using human β-tubulin assay kit (SEB870HU) obtained from (Cloud-Clone Corp. U.S.A.)[16] is performed for some active compounds **4**, **6**, **11**, **13**, **18**, **21**, **23** and **CA-4** against HL 60 cancer cell line to measure the percentage inhibition of β-tubulin polymerization.

Methodology

HL-60 cell line is obtained from American Type Culture Collection, they are cultured using DMEM (Invitrogen/ Life Technologies) supplemented with 10% FBS (Hyclone), 10 mg/mL of insulin (Sigma), and 1% penicillin-streptomycin. Plate cells (cells density 1.2–1.8×10000 cells/well) in a vol-ume of 100 mL complete growth medium and 100 mL of the tested compounds per well in a 96-well plate for 18–24h before the enzyme assay for β-tubulin. The microtiter plate provided in this kit has been pre-coated with an antibody specific to TUBβ. Standards or samples are then added to the appropriate microtiter plate wells with a biotin-conjugated antibody specific to TUBβ. Next, Avidin conjugated to horse-radish peroxidase (HRP) is added to each microplate well and incubated. After TMB substrate solution is added, only those wells that contain TUBβ, biotin-conjugated antibody and enzyme-conjugated Avidin will exhibit a change in color. The enzyme -substrate reaction is terminated by the addition of sulphuric acid solution and the color change is measured spectrophotometrically at a wavelength of 50 nm±10 nm. The concentration of TUBβ in the samples is then determined by comparing the O.D. of the samples to the standard curve. Each experiment was repeated two times (Table 4).

In Vitro ELISA Immunoassay of Apoptosis Mediators.

Materials

The levels of p53, Bax, Bcl-2, caspase-3 and survivin were assessed using ELISA colorimetric kits. All the procedures were performed according to the manufacturer's instructions, Sigma p53 ELISA Human (RAB0500).[51] DRG® Human Bax ELISA (EIA-4487) Marburg, Germany.[52] Bcl-2 ELISA Kit Invitrogen Corporation 1600 Faraday Avenue Carlsbad.[53] Caspase-3 Invitrogen EIA kit Human (active) KHO1091 Invitrogen Corporation 1600 Faraday Avenue Carlsbad.[54] Cloud clone Survivin (Active) eiakit, Cloud clone, Houston, U.S.A..[55]

Methodology

The main principle of sandwich ELISA is the quantification of a specific protein through its containment in a sandwich of specific antibodies conjugated to the colorimetric TMB substrate, whose intensity is proportional to the protein quan-tity and is measured spectrophotometrically. The cell lysate is diluted 10 times, and 100 mL (50 mg protein) is added to the wells of separate micro titer plates for the ELISA kits that are precoated with primary antibodies specific to p53, Bax, Bcl-2, caspase-3, Survivin. A secondary biotin-linked anti-body specific to the protein captured by the primary antibody is added to bind the captured protein, forming a "sandwich" of specific antibodies around the desired protein in the cell lysate. The streptavidin- HRP complex is then used to bind the biotin-linked secondary antibody through its streptavidin por-tion. The HRP domain reacted with the added TMB substrate, forming a colored product that is measured at 450 nm by a plate reader (ChroMate-4300, FL, U.S.A.) after the reaction is terminated by the addition of stop solution.

Acknowledgments The authors thank Dr. Esam Rashwan, Head of the confirmatory diagnostic unit VACSERA-EGYPT, for carrying out the cytotoxicity screening. Authors thank for Dr. Enas. Ahmed Mohamed, associate professor of Anatomy and Embryology, Faculty of Medicine, Cairo University for carrying out tubulin immunofluorescence assay.

Conflict of Interest The authors declare no conflict of interest.

References

1) Fitzmaurice C., Dicker D., Pain A., Hamavid H., Moradi-Lakeh M., MacIntyre M. F., Hamadeh R. R., *JAMA Oncol*, **1**, 505–527 (2015).
2) Akinduro O., Weber T. S., Ang H., Haltalli M. L. R., Ruivo N., Duarte D., Rashidi N. M., Hawkins E. D., Duffy K. R., Celso C. L., *Nat. Commun.*, **9**, 519 (2018).

3) Jabir N. R., Tabrez S., Ashraf G. M., Shakil S., Damanhouri G. A., Kamal M. A., *Int. J. Nanomed.*, **7**, 4391–4408 (2012).
4) Desbène S., Giorgi-Renault S., *Curr. Med. Chem. Anticancer Agents*, **2**, 71–90 (2002).
5) Mendelsohn B. A., Barnscher S. D., Snyder J. T., An Z., Dodd J. M., Dugal-Tessier J., *Bioconjug. Chem.*, **28**, 371–381 (2017).
6) Chen H., Lin Z., Arnst K. E., Miller D. D., Li W., *Molecules*, **22**, 1281 (2017).
7) Shi J., Mitchison T. J., *Endocr. Relat. Cancer*, **24**, T83–T96 (2017).
8) Masawang K., Pedro M., Cidade H., Reis R. M., Neves M. P., Cor-rêa A. G., Pinto M. M., *Toxicol. Lett.*, **229**, 393–401 (2014).
9) Prota A. E., Danel F., Bachmann F., Bargsten K., Buey R. M., Pohlmann J., Steinmetz M. O., *J. Mol. Biol.*, **426**, 1848–1860 (2014).
10) Van Vuuren R. J., Visagie M. H., Theron A. E., Joubert A. M., *Cancer Chemother. Pharmacol.*, **76**, 1101–1112 (2015).
11) Gradishar W. J., *Breast Cancer, Basic a Clinical Research*, **6**, 159–171 (2012).
12) Greene L. M., Nathwani S. M., Bright S. A., Fayne D., Croke A., Gagliardi M., O'Boyle N. M., *J. Pharmacol. Exp. Ther.*, **335**, 302–313 (2010).
13) Zheng S., Zhong Q., Mottamal M., Zhang Q., Zhang C., Le Melle E., Wang G., *J. Med. Chem.*, **57**, 3369–3381 (2014).
14) Romagnoli R., Baraldi P. G., Cruz-Lopez O., Lopez Cara C., Car-rion M. D., Brancale A., Viola G., *J. Med. Chem.*, **53**, 4248–4258 (2010).
15) El-Meligie S., Taher A. T., Kamal A. M., Youssef A., *Eur. J. Med. Chem.*, **126**, 52–60 (2017).
16) El Meligie S., Taher A. T., Khalil N. A., El-said A. H., *Arch. Pharm. Res.*, **40**, 13–24 (2017).
17) ElMeligie S., Khalil N. A., Ahmed E. M., Emam S. H., Zaitone S. A. B., *Biol. Pharm. Bull.*, **39**, 1611–1622 (2016).
18) Abd-El Hameid M. K., Aboul-magd A., Kandeel M. M., El Meligie S., *I.J.M.P.S.*, **3**, 63–74 (2013).
19) Gaukroger K., Hadfield J. A., Lawrence N. J., Nolan S., McGown A. T., *Org. Biomol. Chem.*, **1**, 3033–3037 (2003).
20) Schimmer A. D., *Cancer Res.*, **64**, 7183–7190 (2004).
21) Chandele A., Prasad V., Jagtap J. C., Shukla R., Shastry P. R., *Neoplasia*, **6**, 29–40 (2004).
22) Carter B. Z., Milella M., Altieri D. C., Andreeff M., *Blood*, **97**, 2784–2790 (2001).
23) Nassar A., Lawson D., Cotsonis G., Cohen C., *Appl. Immunohistochem. Mol. Morphol.*, **16**, 113–120 (2008).
24) Li W. L., Lee M. R., Cho M. Y., *Biochem. Biophys. Res. Commun.*, **471**, 309–314 (2016).
25) Abadi A. H., Abouel-Ella D. A., Lehmann J., Tinsley H. N., Gary B. D., Piazza G. A., Abdel-Fattah M. A., *Eur. J. Med. Chem.*, **45**, 90–97 (2010).
26) Hu C. M. J., Zhang L., *Biochem. Pharmacol.*, **83**, 1104–1111 (2012).
27) Markman J. L., Rekechenetskiy A., Holler E., Ljubimova J. Y., *Adv. Drug Deliv. Rev.*, **65**, 1866–1879 (2013).
28) Nepali K., Sharma S., Sharma M., Bedi P. M. S., Dhar K. L., *Eur. J. Med. Chem.*, **77**, 422–487 (2014).
29) Zhang X., Kong Y., Zhang J., Su M., Zhou Y., Zang Y., Lu W., *Eur. J. Med. Chem.*, **95**, 127–135 (2015).
30) Botta M., Forli S., Magnani M., Manetti F., *Top. Curr. Chem.*, **286**, 279–328 (2008).
31) Cheung C. H. A., Chen H. H., Kuo C. C., Chang C. Y., Coumar M. S., Hsieh H. P., Chang J. Y., *Mol. Cancer*, **8**, 43 (2009).
32) Ravichandran S., Karthikeyan E., *Int. J. ChemTech. Res.*, **3**, 466– 470 (2011).
33) Tatke P., Jaiswal Y., *Res. J. Med. Plant*, **5**, 21–31 (2011).
34) Rao Y. K., Fang S. H., Tzeng Y. M., *Bioorg. Med. Chem.*, **17**, 7909–7914 (2009).
35) Devender P., Neha S., *JPR*, **11**, 71–75 (2012).
36) Manna F., Chimenti F., Bolasco A., Filippelli A., Palla A., Filippelli W., Mercantini R., *Eur. J. Med. Chem.*, **27**, 627–632 (1992).
37) Al-Abdullah E. S., *Molecules*, **16**, 3410–3419 (2011).
38) Abdel-Fattah Mohamed A. O., El-Naggar Mahmoud A. M., Rashied Rasha M. H., Gary Bernard D., Piazza Gary A., Abadi Ashraf H., *Med. Chem.*, **8**, 392–400 (2012).
39) Baluja S., Talaviya R., *Int. J. Pharm. Chem. Biol. Sci.*, **5**, 960–970 (2015).
40) Vishal D. J., Mahendra D. K., Sarita S., *Pelagia Research Library*, **3**, 343–348 (2012).
41) Kachroo M., Panda R., Yadav Y., *Der Pharma Chemica*, **6**, 352–359 (2014).
42) Sharshira E. M., Hamada N. M. M., *Am. J. Org. Chem.*, **2**, 26–31 (2012).
43) Van Meerloo J., Kaspers G. J. L., Cloos J., *Methods Mol. Biol.*, **731**, 237–345 (2011).
44) Simoni D., Grisolia G., Giannini G., Roberti M., Rondanin R., Piccagli L., Grimaudo S., *J. Med. Chem.*, **48**, 723–736 (2005).
45) Nihei Y., Suzuki M., Okano A., Tsuji T., Akiyama Y., Tsuruo T., Sato Y., *Jpn. J. Cancer Res.*, **90**, 1387–1395 (1999).
46) Romagnoli R., Baraldi P. G., Cara C. L., Salvador M. K., Bortolozzi R., Basso G., Li J., *Eur. J. Med. Chem.*, **46**, 6015–6024 (2011).
47) Hassan M., Watari H., Abu Al maaty A., Ohba Y., Sakuragi N., *BioMed Res. Int.*, **2014**, 1–23 (2014).
48) Bucur O., Ray S., Bucur M. C., Almasan A., *Front. Biosci.*, **11**, 1549–1568 (2006).
49) Shi Z., Liang Y. J., Chen Z. S., Wang X. H., Ding Y., Chen L. M., Fu L. W., *Oncol. Rep.*, **17**, 969–976 (2007).
50) Patel R. V., Patel P. K., Kumari P., Rajani D. P., Chikhalia K. H., *Eur. J. Med. Chem.*, **53**, 41–51 (2012).
51) Tseng S. J., Liao Z. X., Kao S. H., Zeng Y. F., Huang K. Y., Li H. J., Yang P. C., Deng Y.-F., Huang C.-F., Yang S.-C., Yang P.-C., Kempson I. M., *Nat. Commun.*, **6**, 1–9 (2015).
52) Teijido O., Ganesan Y. T., Llanos R., Peton A., Utrecht J. B., So-prani A., Dejean L. A., *Anal. Biochem.*, **497**, 90–94 (2016).
53) Keerthy H. K., Garg M., Mohan C. D., Madan V., Kanojia D., Shobith R., Koeffler H. P., *PLOS ONE*, **9**, e107118 (2014).
54) Song T., Choi C. H., Cho Y. J., Sung C. O., Song S. Y., Kim T. J., Kim B. G., *Gynecol. Oncol.*, **125**, 427–432 (2012).
55) Nigam J., Chandra A., Kazmi H. R., Singh A., Gupta V., Parmar D., Srivastava M. K., *Med. Oncol.*, **31**, 167 (2014).